

# Multi-Antenna Physical Layer Models for Wireless Network Design

A Thesis  
Presented to  
The Academic Faculty

by

**Hemabh Shekhar**

In Partial Fulfillment  
of the Requirements for the Degree  
Doctor of Philosophy in Electrical and Computer Engineering

School of Electrical and Computer Engineering  
Georgia Institute of Technology  
April 2008

# Multi-Antenna Physical Layer Models for Wireless Network Design

Approved by:

Professor Mary Ann Ingram, Advisor  
School of Electrical and Computer  
Engineering  
*Georgia Institute of Technology*

Professor Henry Owen  
School of Electrical and Computer  
Engineering  
*Georgia Institute of Technology*

Professor Raghupathy Sivakumar  
School of Electrical and Computer  
Engineering  
*Georgia Institute of Technology*

Professor Alfred Andrew  
School of Mathematics  
*Georgia Institute of Technology*

Professor John Copeland  
School of Electrical and Computer  
Engineering  
*Georgia Institute of Technology*

Date Approved: January 2008

*To my parents and brother*

# ACKNOWLEDGEMENTS

I am thankful to my advisor, Prof. Mary Ann Ingram, for providing me an environment to learn and grow not only technically but also as an individual with better discipline, more patience, and perseverance. Her support and encouragement motivated me to continue my research even when I moved out of Georgia Tech and started working before finishing my Ph.D. Also, I would like to thank my committee members: Prof. Raghupathy Sivakumar, Prof. John Copeland, Prof. Henry Owen, and Prof. Alfred Andrew. I especially appreciate the efforts Professors Sivakumar and Copeland for reading this thesis.

I would like to thank my lab members, Sudhanshu Gaur, Vikram Anreddy, Lu Dong, and Guillermo Acosta for making the work environment in the lab very enjoyable. I extend special thanks to Sudhanshu and Guru for technical discussions that helped me get some nice ideas for my thesis. Ms. Cordai Farrar was of immense help in distributing copies of my thesis to the committee members.

My friends Masood-ur Rahman and Abhinav Saxena, were always encouraging and motivating me to focus and work hard on my thesis while I was working at ArrayComm. Their encouragement certainly helped me finish my thesis sooner. Todd Chauvin, my manager at ArrayComm, and John Dogan, research fellow at ArrayComm, kept pushing me to finish my Ph.D. faster, which certainly helped. I thank Todd for being very understanding and allowing me to take time off from work to work on my thesis.

Finally, I would like to acknowledge my parents, brother, and all the relatives for their endless support and encouragement.

Hemabh Shekhar

# TABLE OF CONTENTS

<b>DEDICATION</b> . . . . .	<b>iii</b>
<b>ACKNOWLEDGEMENTS</b> . . . . .	<b>iv</b>
<b>LIST OF FIGURES</b> . . . . .	<b>viii</b>
<b>ABBREVIATIONS</b> . . . . .	<b>x</b>
<b>SUMMARY</b> . . . . .	<b>xi</b>
<b>I INTRODUCTION</b> . . . . .	<b>1</b>
1.1 Evolution of Wireless Networks . . . . .	1
1.2 Advanced Physical Layer . . . . .	5
1.3 Medium Access Control Layer . . . . .	7
1.4 Research Contributions . . . . .	8
1.5 Thesis Outline . . . . .	9
<b>II BACKGROUND</b> . . . . .	<b>10</b>
2.1 Physical Layer Design . . . . .	10
2.1.1 Receiver Designs . . . . .	11
2.1.2 Transmit Strategies . . . . .	13
2.1.3 Single-carrier and Multi-carrier Systems . . . . .	15
2.1.4 Exponential Effective SIR Mapping . . . . .	17
2.2 Medium Access Control Layer Design . . . . .	18
2.2.1 S-Aloha Protocol . . . . .	19
2.2.2 CSMA/CA Protocol . . . . .	19
2.3 Summary . . . . .	20
<b>III COLLISION MODELS FOR LINEAR AND NON-LINEAR RE- CEIVERS</b> . . . . .	<b>21</b>
3.1 Overview . . . . .	21
3.2 Performance Analysis of LMMSE Receiver . . . . .	23
3.3 Average Eigenvalue(s) of a Random Matrix . . . . .	26

3.4	Collision models . . . . .	34
3.4.1	SINR-based collision models . . . . .	34
3.4.2	ABER-based collision models . . . . .	36
3.5	Summary . . . . .	38
3.6	Appendix 3.6: Average Eigenvalues of Wishart Matrix . . . . .	38
3.7	Appendix 3.7: Analytical expression of (48) . . . . .	40
<b>IV</b>	<b>RANDOM ACCESS NETWORK - SINGLE CARRIER . . . . .</b>	<b>42</b>
4.1	Overview . . . . .	42
4.2	Network Model . . . . .	44
4.3	Simulation and Results . . . . .	45
4.4	Summary . . . . .	50
<b>V</b>	<b>RANDOM ACCESS NETWORK - MULTI-CARRIER . . . . .</b>	<b>52</b>
5.1	Introduction . . . . .	52
5.2	Background . . . . .	54
5.2.1	PB Algorithm for Single Channel S-Aloha . . . . .	54
5.2.2	PB Algorithm for Multi-Channel S-Aloha . . . . .	55
5.2.3	Performance Analysis Without Capture . . . . .	55
5.3	Stabilized MC-Aloha with Capture . . . . .	58
5.3.1	Single Packet Reception . . . . .	59
5.3.2	Multi-Packet Reception . . . . .	59
5.3.3	Performance analysis . . . . .	62
5.4	Results . . . . .	63
5.5	Summary . . . . .	66
5.6	Appendix 5.6 . . . . .	66
5.7	Appendix 5.7 . . . . .	69
<b>VI</b>	<b>AD HOC NETWORKS . . . . .</b>	<b>70</b>
6.1	Overview . . . . .	70
6.2	Collision models . . . . .	73

6.2.1	Simple MAC (S-MAC) protocol . . . . .	77
6.2.2	CSMA/CA( $k$ ) MAC protocol . . . . .	78
6.3	Simulation and results . . . . .	79
6.4	Summary . . . . .	81
<b>VII</b>	<b>SUMMARY AND FUTURE RESEARCH . . . . .</b>	<b>83</b>
7.1	Research Summary . . . . .	83
7.2	Future work . . . . .	85
	<b>REFERENCES . . . . .</b>	<b>87</b>
	<b>VITA . . . . .</b>	<b>94</b>

# LIST OF FIGURES

Figure 1	Block diagram of a successive interference cancelation receiver . . .	13
Figure 2	Illustration of spatial multiplexing and space division multiple access	14
Figure 3	Block diagram of an OFDM system . . . . .	16
Figure 4	Average eigenvalues for $a_1 = 5\text{dB}$ using different computation methods, $L = 2$ and $M = 4$ . . . . .	29
Figure 5	Average eigenvalues for $a_1 = 30\text{dB}$ , $L = 2$ and $M = 2, 4, 6$ using approximate CFE and Monte Carlo simulations . . . . .	30
Figure 6	Error (in dB) between the approximation and the values obtained using Monte Carlo simulation, of the eigenvalue for $L = 2$ , $M = 2, 4$ , and $6$ . . . . .	31
Figure 7	Error (in dB) between the approximation and the Monte Carlo simulation values of the eigenvalue for $L = 2$ , $M = 4$ , and parameterized on $10 \times \log(a_1 a_2)$ . . . . .	32
Figure 8	No-capture probability with desired user and two interferers having the same SNR and the threshold, $\gamma_{th} = 9.12\text{ dB}$ . . . . .	32
Figure 9	ABER for LMMSE receiver using Pham's approach [52] and the proposed CFE . . . . .	33
Figure 10	Throughput of S-Aloha network employing two antenna LMMSE receiver obtained using SINR-based collision model with different capture thresholds . . . . .	46
Figure 11	Throughput comparison between S-Aloha networks employing either two antenna LMMSE receiver or a single antenna receiver using SINR-based collision model . . . . .	47
Figure 12	Throughput of S-Aloha network, employing two antenna LMMSE receiver, obtained using ABER-based collision model at $20\text{ dB}$ SNR for different modulations and equal packet length. . . . .	48
Figure 13	ABER-based collision model parameterized on SNR, BPSK modulation, $L = 128\text{ bits}$ . . . . .	49
Figure 14	ABER collision model without coding, parameterized on packet length for BPSK modulation . . . . .	50
Figure 15	Frame structure for MUD . . . . .	60
Figure 16	Average throughput of multichannel S-ALOHA network with (solid and dashed lines) and without (dash-dotted line) capture for SPR. . . . .	63

Figure 17	Average delay of multichannel S-ALOHA network with (solid and dashed lines) and without (dash-dotted line) capture for SPR. . . .	64
Figure 18	Average throughput of multichannel S-Aloha with multiuser detection. Scheme - 1: Decimated preamble, Scheme - 2: Orthogonal training sequences . . . . .	65
Figure 19	Average delay of multichannel S-Aloha with multiuser detection . .	65
Figure 20	Interference scenario in ad-hoc wireless system with V-BLAST transmitters . . . . .	74
Figure 21	Collision model flow chart . . . . .	74
Figure 22	Illustration of the two MAC protocols . . . . .	77
Figure 23	Throughput of an ad-hoc wireless network employing ideal, SIC, and LMMSE receivers with CPPS power scheme . . . . .	81
Figure 24	Throughput of an ad-hoc wireless network employing ideal, SIC, and LMMSE receivers with CPPN power scheme . . . . .	82

# ABBREVIATIONS

AF	Amplify and Forward
AFD	Average Fade Duration
AOD	Average Outage Duration
AR	Auto-regressive
BER	Bit Error Rate
BPSK	Binary Phase Shift Keying
BS	Base Station
CE	Channel Estimation
DF	Decode and Forward
FoO	Frequency of Outage
IFFT	Inverse Fast Fourier Transform
LCR	Level Crossing Rate
LMMSE	Linear Minimum Mean Square Error
LOS	Line of Sight
MEDS	Method of Exact Doppler Spread
MIMO	Multiple-input multiple-output
MMSE	Minimum Mean Square Error
MS	Mobile Station
PSAM	Pilot Symbol Aided Modulation
Rx	Receiver
SoS	Sum-of-sinusoids
SNR	Singal-to-noise Ratio
STBC	Space Time Block Code
Tx	Transmitter

# SUMMARY

The wireless technology is rapidly evolving and involves advanced physical (PHY) and medium access control (MAC) layer designs. Examples of such technologies are 802.16e (mobile single hop WiMAX), 802.16j (mobile multi-hop or mesh WiMAX), 802.11n, 3GPP-LTE, etc. All these technologies require multiple antenna base stations or access points. In some cases even the subscriber stations are required to have multiple antennas. Adding more antennas to the station implies, in most designs, additional RF chains that are quite expensive. It also causes logistical issues at the base stations because of space and strength constraints at the base station towers. These factors necessitate evaluation of the technology before building them for deployment or even trials.

One of the common evaluation methodologies is developing network simulators that model the PHY and MAC layers. Tools such as OPNET and NS-2 are used to develop such network simulators. Another technique is to develop analytical models of the network. However, such models have a limited scope because not all the aspects of PHY and MAC can be easily modeled analytically. In both the methodologies, i.e. developing network simulators or analytical models, the effect of PHY layer is captured by abstraction of the PHY algorithms; this abstraction is also called collision model (CM).

In this thesis, CMs of linear and non-linear multiple antenna receivers, in particular linear minimum mean squared error (LMMSE) and LMMSE with decision feedback (LMMSE-DF), are developed. To develop these CMs, first a simple analytical expression of the distribution of the post processing signal to interference and

noise (SINR) of an LMMSE receiver is developed. This expression is then used to develop SINR- and ABER-based CMs. However, the analytical forms of these CMs are derived only for the following scenarios: (i) any number of receive antennas with three users having arbitrary received powers and (ii) two antenna receiver with arbitrary number of equal received power users. For all the other scenarios a semi-analytical CM is used.

The PHY abstractions or CMs are next used in the evaluation of a random access cellular network and an ad hoc network. Analytical model of the random access cellular network is developed using the SINR- and ABER-based CM of the LMMSE receiver. The impact of receiver processing is measured in terms of throughput. In this case, the random access mechanism is modeled by a single channel S-Aloha channel access scheme. Another analytical model is developed for single and multi-packet reception in a multi-channel S-Aloha channel access. An *ideal* receiver is modeled in this case, i.e. the packet(s) are successfully received as long as the total number of colliding packets is not greater than the number of antennas. Throughput and delay are used as performance metrics to study the impact of different PHY designs.

Finally, the SINR-based semi-analytical CMs of LMMSE and LMMSE-DF are used to evaluate the performance of multi-hop ad hoc networks. Throughput is used as the performance evaluation metric. A novel MAC, called S-MAC, is proposed and its performance is compared against another MAC for wireless networks, called CSMA/CA( $k$ ).

# CHAPTER I

## INTRODUCTION

### *1.1 Evolution of Wireless Networks*

The evolution of wireless network has drastically changed the world of communication. Wireless systems have evolved from simple network designs with low data rate and reliability to much intricate designs supporting very high data rate and reliability. This transition has been possible because of technological advancements in the hardware and the desire for high data rate wireless applications. The first wireless network was developed at the University of Hawaii under the guidance of Dr. N. Abramson [7], [20]. This network is the popularly known Aloha system. The original goal of the Aloha system was to investigate the use of radio communication as an alternative to telephone system for computer communication. This was because in late 1960s telephone networks were being used for information transfer among different computers. The then existing telephone networks were not suited for rapidly emerging data networking needs.

The principle on which an Aloha-based network worked was that transmissions were done whenever there was a packet available at the nodes. Subsequently, a modified version known as Slotted Aloha (S Aloha) was developed [20], [48], [12]. This modification divided transmissions in equal length periods called Slots, and all the nodes are synchronized to begin transmitting only at the beginning of a Slot. This required all the packets to be of the same duration in S-Aloha. This modification doubled the network throughput.

A better understanding of the performance of an S-Aloha system requires a theoretical model of the Physical (PHY) and Medium Access Control (MAC) layers.

Greater accuracy in the theoretical model results in better performance predictions. The theoretical model of MAC layer of S-Aloha systems is simple. This allows a tractable system model while using an advanced PHY layer model. The insight gained from detailed analysis of the S-Aloha networks helps in the evolution of new and more complicated networks like cellular and mesh. S-Aloha based random access techniques are used in practical systems for control signalling [24] and [2] and data communication [5], [57], and [73].

Although the S-Aloha systems were very popular, their throughput was limited because of the inherent limitation of the random access channels caused by user collision. It was obvious that by coordinating the channel access of the users in the network, throughput can be improved. A cellular network with a base station having centralized control of the channel access can reduce the collision. The concept of cellular communication was first demonstrated by Bell Labs in 1947, but cellular systems evolved commercially in late 1970s. The second generation or 2G cellular systems evolved to a completely digital form. Time Division Multiple Access (TDMA) and Code Division Multiple Access (CDMA) were two main technologies that constituted 2G systems. Global System for Mobile (GSM) communication and IS-95 are the examples of TDMA- and CDMA-based standards, respectively.

The third generation or 3G system is a significant advancement over 2G. and consequently requires a more advanced models of the PHY layer. The 3G systems use Wideband CDMA (WCDMA) technology and promise support of up to 2 Mbps data rate for data and multimedia in addition to voice traffic. This is a significant advancement over 2G systems, which can support only up to 14.4 Kbps data rate for data and voice traffic. Research is underway to enhance the system efficiency even further. A significant increase in the data traffic rate up to 100 Mbps is targeted. Such research requires good theoretical and simulation based models. Rigorous theoretical models for such a network are difficult to derive. Most researchers use S-Aloha based

models for such studies, since they offer reasonable insights in to the performance of cellular networks [5-8]. The simulation based models give more realistic performance. However, both theoretical- and simulation-based models are critically dependent on the quality of PHY layer abstraction utilized. The PHY layer becomes more and more sophisticated because of the involvement of the latest technologies like multiple antennas, space time coding, etc. As a result, a simple PHY layer abstraction is not accurate for simulation models. This thesis addresses the challenge of deriving an accurate PHY layer abstraction for certain types of multi-antenna transmitters and receivers.

Another type of wireless network in the evolution cycle is the Wireless Local Area Network (WLAN). The IEEE 802.11 standard [3] that specifies details of WLAN design was first published in 1997. Initial systems were designed with single transmit antenna (IEEE 802.11a/b/g). When multiple transmit antennas at a node became a reality, a new standard (IEEE 802.11n) was set and it continues to evolve. While its predecessors supported up to 54 Mbps, 802.11n promises data rates exceeding 100 Mbps. Such a high data rate has created or motivated new directions of research in wireless home networking. Multiple devices in a home network can have a high data rate wireless connection for applications like video streaming, HDTV over home network, etc. The challenge still remains with the design choices of PHY layer because of differences of opinion in the groups of companies. One group suggests V-BLAST-type transmission for higher data rate, while another suggests Alamouti-based space time coding for higher data reliability along with greater number of antennas for higher data rate. Industrial research in this direction is based on network level simulations using OPNET. However, a better PHY layer abstraction is needed to understand the effect of using different PHY layers.

Ad hoc and mesh networks are other forms of wireless networks that are attracting attention now. An ad hoc network, as the name suggests, is formed of nodes that join

or leave the network on the fly and do not require any pre-installed infrastructure. The types of ad hoc networks ranges from small static networks to large scale highly dynamic ones. Dynamic communication for disaster relief efforts, battlefield networks, etc. requires ad hoc networks. Such network scenarios cannot rely on centralized and organized connectivity. The growth of ad hoc networks is at a very nascent stage. The IEEE 802.11(a/b/g) wireless Medium Access Control (MAC) protocol incorporates an ad hoc networking system when no access point is present. However, this is a very basic ad hoc MAC protocol, as it assumes all nodes are within decoding range of each other. Such a network is said to have a single hop communication. Each node transmits and receives data of its interest but does not route other users' data between the network's systems. When the nodes not only transmit or receive the packets of their interest but also of other users in the network, the network is said to have a multi-hop communication. Performance of a multi-hop ad hoc network has caught the interest of the wireless research community at PHY as well as higher layers.

Finally, the development of mesh networks is an attempt towards seamless broadband connectivity. The IEEE 802.16 (WiMAX) [2] and the IEEE 802.20 (MobileFi) standards are focused towards broadband networks. Both the standards have guidelines for mesh networking. The underlying idea behind the mesh networks is to connect different types of network with the aid of WiMAX base stations that will support multi-hop communication and a pre-defined Quality-of-Service (QoS) required for mesh networks. This IP-based wireless broadband technology can be integrated with 3G mobile networks, 802.11-based WLANs, and wireline networks to provide seamless broadband connectivity to mobile users.

The establishment of the wireless mobile networks discussed above is technically very challenging. Motivated by the need to provide a greater level of adaptation to variations of wireless channels, this thesis proposes to:

- i) provide an advanced model for physical layer signal processing, modulation, and coding and
- ii) design MAC and joint MAC/PHY protocols for substantially enhancing data rate and reliability of wireless packet networks.

The following two sections introduce the advanced PHY layer technologies and MAC protocols that can be used in the next generation networks like 4G and WiMAX.

## ***1.2 Advanced Physical Layer***

Two decades ago the wireless systems were designed with single antenna transceivers. Introduction of multiple antenna transceivers have revolutionized wireless research, not only at the PHY layer but also at the MAC and higher layers. Owing to its capability to provide higher data rate and reliability, multiple antenna transceivers offer a continuum of choices at the transmitters and receivers that support performance from high rate to high reliability. These choices will be discussed briefly in this section.

Multiple antennas at the receiver can be used with different processing and supporting hardware to give a range of designs and levels of performance. Typical designs include phased array, adaptive beam-former, linear and non-linear interference canceller, and Spatio-Temporal Adaptive Processor (STAP). This list is in an increasing order of complexity.

A phased array receiver [70] requires a set of complex weights (equal to the number of antennas) that steer the antenna pattern in desired direction. This design has only one degree of freedom (DoF), the steering angle. An adaptive beam-former [29], [70], and [76] as the name suggests, has an adaptive antenna pattern. All the complex weights in this design can be independently adjusted based on the channel condition. The number of DoFs for this design is equal to the number of antennas. This means that an M-antenna receiver can receive one desired user while suppressing up to M-1 interferers by placing the nulls in their direction of arrival [76]. Suppressing each

interferer requires one DoF, thereby reducing the diversity order of the system by the number of suppressed interferers [76]. The diversity order of a system is a reflection of the link reliability - higher diversity order implies higher reliability.

The linear interference cancellers (LICs) are receivers that use linear processing to suppress interference. Some examples of linear processing are Linear Minimum Mean Squared Error (LMMSE), Zero Forcing (ZF) and maximum Signal-to-Interference plus Noise Ratio (SINR) [70]. An adaptive beamformer also falls into the category of LIC.

A Non-Linear Interference Canceller (NLIC) consists of a feed-forward filter followed by a feedback filter [26]. The feed-forward block performs linear operation to suppress the interferer and the feedback filter cancels the interfering signals by subtracting them out after demodulation. The demodulation step is the non-linear part of interference cancellation (IC). Broadband signals that experience frequency selective fading can benefit from information in the multipath along with the spatial diversity because of multiple antennas. Another form of linear receiver that exploits both space and time diversity is called a space time adaptive processor (STAP) [37]. A STAP processor extracts additional DoFs from the temporal domain and uses it for interference suppression.

The way multiple antennas at the transmitter are used can be classified, based on (i) availability of the channel state information (CSI) at the transmitter and (ii) rate and reliability performance. The first classification requires a feedback path from the receiver to make the CSI (full or partial) [39] available at the transmitter. In this case the system is called “closed loop”; an example of which is diagonal-BLAST (D-BLAST) [17]. When the CSI is not available at the transmitter the system is called “open loop” an example of this type of a system is vertical-BLAST (V-BLAST) [17] and [53]. In the second classification, a higher rate is achieved when different antennas transmit more than one linearly independent stream of data, simultaneously.

D-BLAST and V-BLAST are examples of such high rate systems. Higher reliability is achieved by introducing redundancy in space, e.g. transmit beam-forming, or in both space and time, e.g. Space Time Block Codes (STBC). It should be noted that the transmit beam-forming is a special case of D-BLAST when only the strongest eigen-mode is used for transmission. Hence, we realize that using multiple antennas in a closed loop system results in rate and reliability improvement at the expense of added complexity of a feedback channel, which is not trivial. It should also be noted that using a higher rate transmission (greater than one stream) requires multiple antennas at the receiver(s) as well.

Many researchers who study the performance of the different kinds of networks discussed in Section 1.1 with multiple antennas, use simplistic abstraction of the PHY layer. Such PHY layer abstractions are also called *Collision Models* (CMs). In this dissertation, we develop Collision Models for LIC and NLIC receivers.

### ***1.3 Medium Access Control Layer***

The MAC layer is responsible for controlling the access of a node to the wireless channel and ensuring the desired QoS parameters like throughput, delay, jitter, etc. Design of a good MAC protocol is crucial for systems using multiple antennas. As discussed in Section 1.1, the network architectures can be broadly divided into two categories, ad hoc and cellular. Design of an advanced MAC for an ad hoc network with multiple antennas is a difficult problem because of the decentralized nature of the protocol required.

The simplest design for single-input-single-output (SISO) systems is called Collision Sense Multiple Access with Collision Avoidance (CSMA/CA) [12]. The CSMA/CA protocol requires a node to first sense the medium before transmitting. If an ongoing transmission is identified, a random back-off is initiated before the next transmission attempt.

A simple extension of CSMA/CA to the Multiple-Input-Multiple-Output (MIMO) case is called CSMA/CA( $k$ ) [31], where  $k$  is the number of antennas at the transmitter. This protocol requires the nodes to transmit using a V-BLAST-type scheme. For this system to be useful, the receiver should have at least  $k$  antennas. Researchers are trying to develop more efficient MAC protocols for ad hoc networks. A new MAC protocol called simple-MAC (S-MAC) is proposed in this dissertation.

Designing a MAC protocol for cellular networks employing multiple antennas is relatively easier because of the centralized control by a base station or an access point. A simple S-Aloha-based MAC protocol captures the essence of the system model comprising MAC and PHY layers. We use this approach for analytical study of the impact of multiple antennas in a cellular network.

## ***1.4 Research Contributions***

- A closed-form CM is developed for the LMMSE receiver in the Rayleigh fading channel [62], [60]. The closed-form CM is developed for the two interferer scenario and an arbitrary number of receiver antennas. The interferers can have disparate received powers.
- A closed-form CM is developed for a two-antenna LMMSE receiver with an arbitrary number of equal-received-power users. This CM is used to derive a closed-form throughput expression for the S-Aloha network [59].
- A semi-analytical CM is developed for arbitrary number of receiver antennas and interferers with disparate received powers. This CM is used to study the throughput of an ad hoc wireless network and an S-Aloha network [59].
- A model is developed for single- and multi-packet reception in a stabilized multichannel S-Aloha network with capture [61], [63].

- A new space division multiple access (SDMA)-based MAC protocol called S-MAC is proposed for ad hoc networks [21]. Effect of linear and non-linear receiver processing in a multi-hop ad hoc network with S-MAC is compared to a V-BLAST based CSMA/CA MAC protocol [31].

## ***1.5 Thesis Outline***

The remainder of the thesis is divided into six chapters. In Chapter II, we provide the necessary background to easily follow this thesis. Chapter III presents SINR- and ABER-based CMs for an LMMSE receiver in Rayleigh fading channel. These CMs will be used with different network models (ad hoc and S-Aloha) to study throughput and delay (only with S-Aloha) performance. In Chapter IV, a framework is developed to study the throughput of S-Aloha network using SINR- and ABER-based CMs. Chapter V presents a different framework of S-Aloha network that allows the study of delay along with throughput performance for different PHY layer parameters. A new MAC protocol for MIMO ad hoc network called S-MAC is proposed and its throughput performance is compared with CSMA/CA(k) in Chapter VI, using the SINR-based CM. Finally, in Chapter VII we conclude by summarizing our research contributions and open areas of research in physical layer modeling for designs of wireless networks.

# CHAPTER II

## BACKGROUND

A few key concepts and the necessary background of the research is discussed in this chapter. As mentioned in the previous chapter, the goal of this research is to develop a physical layer abstraction that will enable better analysis of different wireless networks via simulation or with analytical models.

At the physical layer, linear and non-linear receiver processing are considered. Hence, we begin the discussion of physical layer design in Section 2.1 with basic concepts and the operating principals behind LMMSE, which is a linear receiver, and SIC, which is a non-linear receiver. Next we discuss two transmit strategies of interest, spatial multiplexing (SM) and space division multiple access (SDMA), and their respective tradeoffs. Single- and multi-carrier systems are also discussed. Both linear and non-linear receivers are of great interest in current wireless systems and hence the impact of these advanced physical layer algorithms on systems employing SM and SDMA is evaluated in the thesis.

The background of MAC layer designs for cellular and ad hoc networks is covered in Section 2.2. The cellular system under consideration in this thesis uses the S-Aloha-based random access channel. A brief discussion on S-Aloha system is presented in Section 2.2.1. Next, the main properties of ad hoc networks and MAC protocols particularly for the 802.11 standard are summarized in Section 2.2.2.

Finally, the chapter is summarized in Section 2.3.

### ***2.1 Physical Layer Design***

There are a number of advanced PHY layer algorithms that have been enabled because of multiple antenna receivers. Some of the popular linear receivers are MRC

[75], equal gain combining [67], selection combining [71], LMMSE [76], etc. Examples of popular non-linear receivers are sphere decoder, successive interference cancelers (SIC), parallel interference cancelers (PIC), etc. There are multiple ways of implementing these receivers. However, in this section we will only discuss the MMSE and SIC receivers since they are the most popularly used algorithms because of their lower implementation complexity compared to sphere decoder or PIC. These two receivers are also of prime interest in the thesis.

Let the receiver have  $M$  antennas and let the model of the received signal be

$$\mathbf{x} = \mathbf{u}_0 s_0 + \sum_{i=1}^L \mathbf{u}_i s_i + \mathbf{n}, \quad (1)$$

where  $\mathbf{u}_i$  is an  $M \times 1$  vector of  $i$ -th user channel gain that includes the effects of path loss and short term fading,  $s_i$  is the transmitted symbol of the  $i$ -th user, and  $\mathbf{n}$  is the receiver noise. There are a total of  $L$  interferers and the desired user always has index zero without any loss of generality.

### 2.1.1 Receiver Designs

The MMSE receiver minimizes the mean squared error between the desired and the combined signal, i.e.

$$J_{min} = \arg \min_{\mathbf{w}} E [ |s_0 - \mathbf{w}^H \mathbf{x}|^2 ] \quad (2)$$

The above expression can be rewritten as

$$J_{min} = \arg \min_{\mathbf{w}} [ (\mathbf{w} - \mathbf{R}_{xx}^{-1} \mathbf{r}_{xd})^H \mathbf{R}_{xx} (\mathbf{w} - \mathbf{R}_{xx}^{-1} \mathbf{r}_{xd}) + R_{dd} - \mathbf{r}_{xd}^H \mathbf{R}_{xx}^{-1} \mathbf{r}_{xd} ], \quad (3)$$

where  $\mathbf{R}_{xx}$  is the covariance matrix of the received signal,  $\mathbf{r}_{xd}$  is the cross correlation matrix between the received signal and  $s_0$  is the desired user signal. Clearly, the weight that minimizes the expression in (3) is

$$\mathbf{w} = \mathbf{R}_{xx}^{-1} \mathbf{r}_{xd}. \quad (4)$$

A useful tool is Woodbury's matrix inversion Lemma [66], which is given as

$$(\mathbf{A} + \mathbf{UCV})^{-1} = \mathbf{A}^{-1} - \mathbf{A}^{-1} \mathbf{U} (\mathbf{C}^{-1} + \mathbf{VA}^{-1} \mathbf{U}) \mathbf{VA}^{-1}, \quad (5)$$

where  $\mathbf{A}$ ,  $\mathbf{U}$ ,  $\mathbf{C}$ , and  $\mathbf{V}$  all denote matrices of the correct size. Now,  $\mathbf{R}_{xx}$  is expanded as  $(\Phi + \mathbf{u}_0\mathbf{u}_0^H)$ , where  $\mathbf{u}_0\mathbf{u}_0^H$  is the spatial covariance matrix of the desired user and  $\Phi$  is the noise plus interference covariance matrix. Using (5) the weight in (4) is re-written in the form

$$\begin{aligned}\mathbf{w} &= \left( \Phi^{-1} - \Phi^{-1}\mathbf{u}_0(1 + \mathbf{u}_0^H\Phi^{-1}\mathbf{u}_0)^{-1}\mathbf{u}_0^H\Phi^{-1} \right) \mathbf{u}_0 \\ &= \frac{1}{1 + \rho} \Phi^{-1}\mathbf{u}_0,\end{aligned}\tag{6}$$

where  $\rho = \mathbf{u}_0^H\Phi^{-1}\mathbf{u}_0$ .

Next, the expression of post processing SINR is discussed. The SINR is given by [47]

$$\gamma = \frac{\mathbf{w}^H\mathbf{u}_0\mathbf{u}_0^H\mathbf{w}}{\mathbf{w}^H\Phi\mathbf{w}}.\tag{7}$$

Substituting (6) for  $\mathbf{w}$  in (7) and applying basic linear algebra operations, another expression of SINR is given as [47]

$$\gamma = \mathbf{u}_0^H\Phi\mathbf{u}_0.\tag{8}$$

Distribution of SINR is most easily derived using this formulation. The following Section presents a few approaches that derive the SINR distribution using (8).

The SIC (or decision feedback) receiver is also considered in this thesis. The effect of this receiver on the performance of an ad hoc network is studied. The receiver may be used as an interference canceler or a multi-user detector (MUD). An interference canceler, as the name suggests, decodes the interfering streams and subtracts them out till the desired user is decoded. A MUD receiver operates in the same way but all the streams are assumed to be from desired user(s). A decision feedback receiver for a narrowband frequency-flat channel is described as follows. Assume the received signal model

$$\mathbf{x} = \mathbf{H}\mathbf{s} + \mathbf{n},\tag{9}$$

where  $\mathbf{x}$  is an  $M \times 1$  received signal,  $\mathbf{H}$  is an  $M \times N$  channel matrix,  $\mathbf{s} = [s_0, s_1, \dots, s_{N-1}]^T$

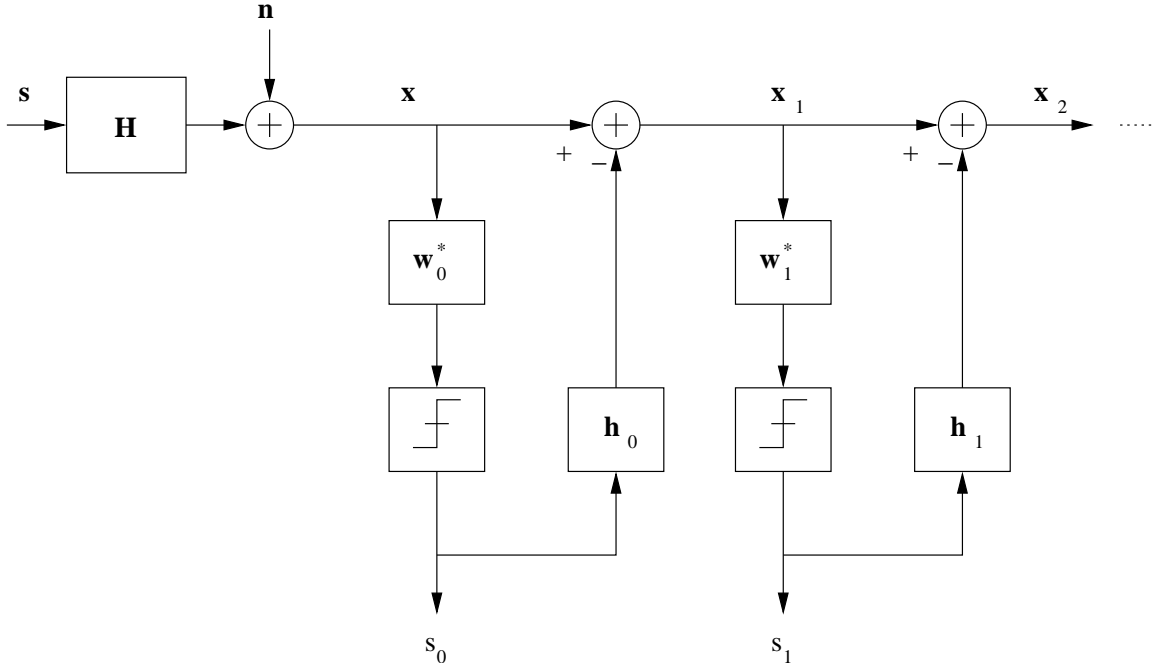


**Figure 1:** Block diagram of a successive interference cancellation receiver

is an  $N \times 1$  transmitted signal vector that is transmitted from  $N$  antennas of a single user, and  $\mathbf{n}$  is an  $M \times 1$  noise vector at the receiver.

Figure 1 shows the block diagram of a SIC receiver. First the decision of  $\hat{s}_0$  about the first symbol is made by slicing the decision statistic  $z_0 = \mathbf{w}_0^H \mathbf{x}$ , where the weight  $\mathbf{w}_0$  is computed as per (4) [26]. This is called the *nulling step*, because beam nulls are formed in the directions of the interferers. Then the contribution of  $\hat{s}_0$  to  $\mathbf{x}$  is reconstructed and subtracted off. This is called the cancellation step because the decoded user is canceled. The process is repeated until the user of interest (in case of IC) or all the users (in case of MUD) are decoded. Performance of SIC can be further improved if the users are decoded in descending order of their received power. This is called a sorted SIC [26].

### 2.1.2 Transmit Strategies

Conventional transmit strategies in wireless communication do not allow multiple streams to be transmitted on the same time and frequency resource. However, the

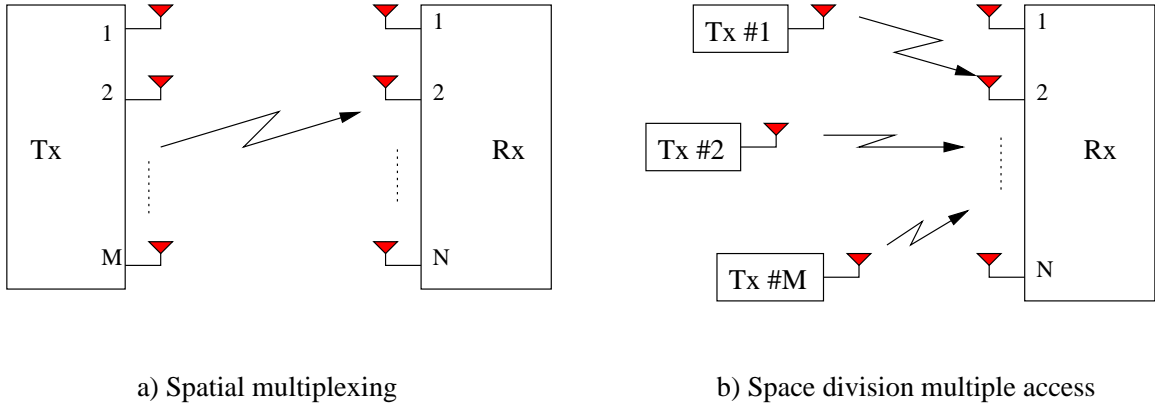


**Figure 2:** Illustration of spatial multiplexing and space division multiple access

multiple antenna receivers, e.g. those discussed in Section 2.1.1, now enable multiple streams to be received simultaneously. Two advanced transmit strategies that are of interest in this thesis are spatial multiplexing (SM) and space division multiple access (SDMA).

In SM, one user transmits more than one stream using multiple antennas. This can be achieved in a number of ways, e.g. D-BLAST, V-BLAST, etc. In the case of V-BLAST, the signal model is the same as (9) with  $s_n$ ,  $0 \leq n < N$ , transmitted from the  $n$ -th antenna. Figure (2)(a) illustrates the SM transmit strategy. As can be seen from (9) multiple symbols are transmitted on the same time and frequency resource, thereby increasing the effective data rate. Spatially multiplexed or MIMO links have received a great deal of attention because of the tremendous spectral efficiencies that can be achieved because of their parallel nature. Specifically, the well-known result (and the great advantage of this approach) is that the capacity increases linearly with the number of transmit and receive antennas in a rich multipath environment [25]. Often, indoor wireless networks and terrestrial military and emergency relief networks have rich multipath channels. The disadvantages of SM are (1) a radio chain is required for each antenna element, and in the closed-loop case, (2) channel information is required at the transmitter, and (3) variable power and bit loading requires more computing complexity at the transmitter than for the other methods. SM also causes

more interference on unintended receivers, hence, reducing their diversity gain or reliability [76].

Another form of multiple stream reception is called SDMA [71], [22], and [35]. Figure 2(b) illustrates the SDMA transmit strategy. In this transmit strategy, multiple users transmit on the same time and frequency resource. The signal model in (9) represents a SDMA strategy when  $s_n$ ,  $0 \leq n < N$  is transmitted by  $n$ -th user. It may be noted that in a more general case each user can transmit more than one stream. For the receivers described earlier to work the best, the SDMA users must have un-correlated channels. This suggests a criterion for user scheduling. The sorted SIC receiver works better when there is power disparity between different users [?]. SDMA provides such a scenario. Hence, it is expected that SDMA and SIC should be a better combination to improve system performance than SM and SIC with equal power streams. This will be investigated in the thesis.

### 2.1.3 Single-carrier and Multi-carrier Systems

Almost all the wireless systems developed till early 90's were single carrier. As the name suggests, a single carrier system is one where information (coded/uncoded) is sent over one carrier per symbol time. A single carrier system may, however, be narrowband or wideband. In this thesis we focus only on the narrowband single carrier system. Mathematically, the base-band model of a narrowband single carrier system is given as

$$x(t) = \sum_{k=-\infty}^{\infty} s(k)h(t - kT) + n(t), \tag{10}$$

where  $T$  is the symbol time,  $s(k)$  is the  $k$ -th transmitted symbol and  $n(t)$  is the receiver noise at time instant  $t$ . Some of the upcoming standards use single-carrier systems, for example 3GPP-LTE uses such a system in the uplink. By definition, in a narrow-band system, the coherence bandwidth of the channel is larger than the signal bandwidth [67]. This results in a frequency-flat fading of the signal. In this

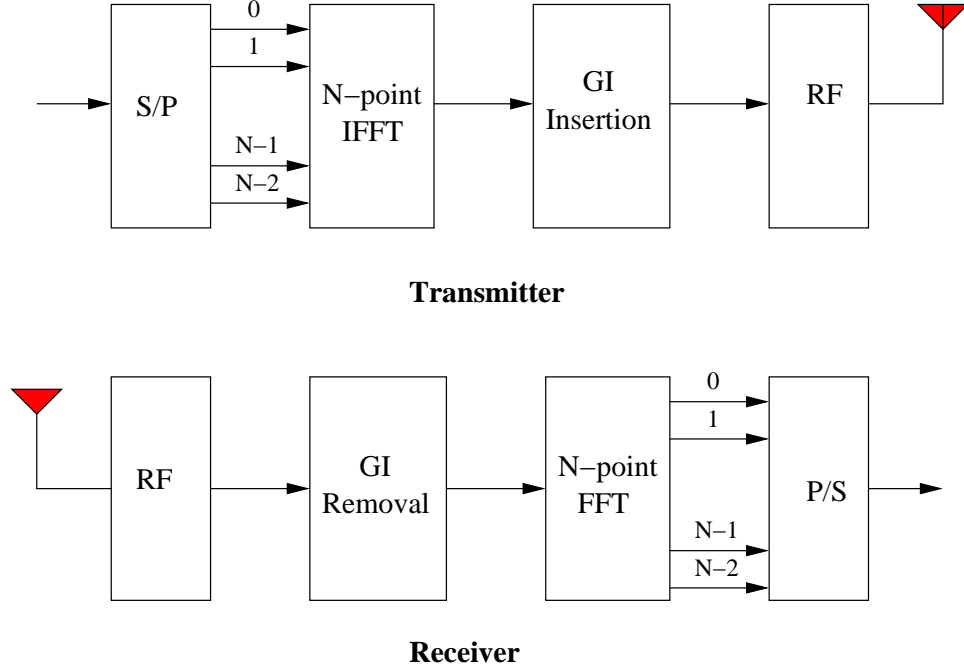


**Figure 3:** Block diagram of an OFDM system

thesis we make this assumption when analyzing narrowband single-carrier systems.

Orthogonal frequency division multiplexing (OFDM) is a popular multi-carrier system that improves the spectral efficiency beyond the traditional frequency division multiplexing (FDM) system [6]. By using an inverse FFT (IFFT) and an FFT to modulate and demodulate data blocks, respectively, OFDM divides the entire channel into many overlapped and orthogonal narrowband subchannels [6],[49]. To protect against ISI in the frequency selective channel, a guard interval (GI) longer than the maximum delay is introduced between successive OFDM symbols. The guard interval is commonly implemented by cyclic extension of the IFFT output, which maintains the orthogonality of the subchannels [6],[49]. The block diagram of the OFDM system is shown in Figure 3. Further advancement in multicarrier systems allows multiple users to access the channel at the same time by using different subsets of sub-carriers, while maintaining orthogonality in the frequency domain. This technique is called orthogonal frequency division multiple access (OFDMA) and it helps in improving the over all network throughput, especially in a data network that has bursty traffic

[71],[25].

#### 2.1.4 Exponential Effective SIR Mapping

A method called exponential effective SIR mapping (EESM) that is accepted across the industry, to evaluate the performance of PHY layer algorithms with different modulation and coding schemes is discussed in this section. A two-step technique is typically followed in industry to capture the effect of the PHY layer with forward error correction (FEC): (i) post processing SINR-based CM of the PHY algorithm and (ii) using this CM in EESM to capture the effect of FEC. Most of the work in this thesis is for uncoded systems. The coded system considered in this thesis uses a one-step technique based on an average bit error rate (ABER)-based CM for a code that can correct up to  $t$  bits of error. The EESM, on the other hand, can be used to approximately model any real FEC code, e.g. turbo code, convolutional code, etc. Although EESM is not used in the this thesis, it is discussed to give the reader an understanding of this technique to model the effect of FEC. It will be a useful to extend the work on uncoded systems in this thesis to incorporate the effect of FEC using the two-step technique to capture the effect of PHY algorithm and FEC.

One of the most time consuming steps at the transmitter and the receiver is error correcting and decoding respectively, making modeling of coders and decoders in network level studies extremely difficult. Also, it is hard to find closed form expressions to capture the code performance reasonably well. Hence, a parameterized approximation has been developed and used by the wireless industry. This is the Exponential Effective SIR Mapping (EESM) [10]. EESM is a method to estimate demodulator performance in a channel with frequency selective signal and/or noise. In a sense, the EESM is a channel-dependent function that maps power level and modulation and coding scheme (MCS) level to SINR values in the Additive White Gaussian Noise (AWGN) channel domain. This allows using this mapping along with

AWGN assumptions (such as effect of an increase in power, CINR/MCS threshold tables) in order to predict the effect of MCS and boosting modification. EESM, given by [74] and [10]

$$\gamma_{eff} = -\beta \ln \frac{1}{N} \sum_{i=1}^N e^{-\frac{\gamma_i}{\beta}}, \quad (11)$$

It is a mapping from the tone SINR's  $\gamma_i$  to an effective SINR  $\gamma_{eff}$ . The parameter  $\beta$  is dependent on the MCS level and has to be calibrated. The mapping is derived from the Chernoff union bound for bit error rates for uncoded Binary Phase-Shift Keying (BPSK) transmissions. Studies have shown that EESM can be extended to different codes and higher modulations by adjusting the parameter  $\beta$  [74]. In this form it could be used to predict FEC block error rates (BLER), both for simulation and as a tool for link adaptation. In simulation EESM could be used to determine throughput using ideal link adaptation without having to simulate coding and decoding. Although this step is not considered in the thesis, it is discussed here for completeness.

## ***2.2 Medium Access Control Layer Design***

Every wireless standard has a MAC layer that provides a variety of functions that support the operation of wireless networks. In general, the MAC layer defines how the users in the network access the shared radio channel. For example, if the MAC uses S-Aloha random access scheme, each subscriber station transmits its packet at the beginning of the slot. Another example is the collision sense multiple access with collision avoidance (CSMA/CA) protocol used in the 802.11 standard to perform the tasks of carrier sensing, transmission, and receiving of 802.11 frames. In the following two sections, a brief discussion is presented on the two protocols, S-Aloha and CSMA/CA, which are considered in this thesis.

### 2.2.1 S-Aloha Protocol

The idealized model of S-Aloha is that a packet is successfully received only when there is no collision [7]. This model allows us to focus on the problem of the contention that occurs when multiple nodes attempt to use the channel simultaneously. In order to model the effect of physical layer algorithms more accurately, abstractions of the desired algorithms are required [28]. Using MUD, more than one co-channel packet can be received successfully in one time slot, thereby increasing the network throughput. Two popularly used preamble designs are used in this thesis to facilitate MUD in an S-Aloha network [58].

Another important aspect of S-Aloha networks is their stability. It is known that the conventional S-Aloha network is unstable when the arrival rate of new packets is large and/or when the packet re-transmission probability is high [55]. A number of stabilization algorithms have been proposed in the literature [19], [23], and [55]. In this thesis we use the pseudo-Bayesian algorithm [65] for modeling and analysis of a stabilized multi-channel S-Aloha network.

### 2.2.2 CSMA/CA Protocol

We are primarily interested in distributed algorithms that can be used by ad hoc networks. A popular MAC scheme in wireless ad hoc networks is the distributed coordination function (DCF) mode of the IEEE 802.11 standard. A simple extension of this MAC for MIMO, called the CSMA/CA(k) scheme, proposed by Karthik et. al in [31] is used as baseline for comparison with the new MAC proposed in this thesis. Therefore, we give a brief discussion of the ad hoc networks and the MAC protocol of 802.11.

Ad hoc networks are multi-hop wireless networks that have no fixed infrastructure and no centralized administration. The mobile stations in the network function as forwarders and participate in the routing process. Nodes communicate by creating a

network “on the fly,” and the topology can change as the nodes move.

The MAC layer is responsible for fair and orderly use of the shared medium. The MAC protocol used in the IEEE 802.11 standard is carrier-sense multiple-access with collision avoidance (CSMA/CA). In this protocol, a node with a packet to be transmitted first listens to ensure no other node is transmitting. If the channel is clear, it transmits the packet. Otherwise, it backs off, and tries again later. The back-off time is randomized to minimize the collisions between packets. When the channel is detected vacant by the carrier-sense method, the transmitter first sends a request-to-send (RTS) message. The recipient answers with a clear-to-send (CTS), if it is not contending. This exchange of control packets aims to ensure collision-free transmission of the data. The transmission of the data packet (DATA) is followed by an acknowledgement (ACK) by the receiver. If the transmitter does not hear the ACK, the data is retransmitted [4].

Suppose two or more nodes have packets to be sent to different receivers in a network. With the TDMA-based MAC protocol, each transmitter would try to gain access to the channel, and only one link would be active at all times. However, with multiple antennas at all nodes, another MAC protocol that exploits the spatial filtering capabilities of the arrays might yield higher throughput.

## ***2.3 Summary***

In this chapter we provided necessary knowledge and background for this research. We first discussed the physical layer aspect of this research that covers linear and non-linear receiver processing, spatial multiplexing and SDMA, and single and multi-carrier systems. Then we discussed two MAC protocols considered in this thesis: i) S-Aloha and ii) CSMA/CA.

## CHAPTER III

# COLLISION MODELS FOR LINEAR AND NON-LINEAR RECEIVERS

### *3.1 Overview*

Array receivers that do linear minimum mean squared error (LMMSE) suppression of interference have been of interest for a long time in the radar and communication literature [70]. Until recently, the cost of such transceivers has precluded their use in user equipment (e.g. handsets, laptops). Now, however, multi-antenna radios are a part of WiMAX [2] and IEEE802.11n [4], and are also of interest in wireless ad hoc networks. The primary tool of analysis for these large networks is simulation using programs such as Opnet and NS-2 [1], [22], [31]. The coarse timescale of a network simulation requires that a wireless link be represented in terms of its outage rate or probability of packet capture simply as a function of the powers and ranges to the desired and interfering sources. This chapter provides such a model in analytical form for a LMMSE receiver when there are two uncorrelated interferers and an arbitrary number of antennas or two antennas and an arbitrary number of equal powered interferers. In semi-analytical form these models can be applied to an arbitrary number of antennas and interferers with different powers. Later in the thesis the collision models developed in this chapter are used for analysis of random access channels and ad hoc networks.

The approach is to first find simple approximations for the respective averages of the first two eigenvalues of the interference covariance matrix, assuming a Rayleigh-fading environment. The average eigenvalues are then applied, via the method of Pham [52], to derive average BER and SINR CDF for the LMMSE receiver. Either of these may then be used to calculate accurate approximations for the PER or packet

capture probability for the link.

Exact expressions for outage probability of SINR and ABER have been found [33]. These exact expressions require multiple evaluations of the hypergeometric functions to obtain the moment generating function (MGF), which are then used to compute the outage probability using the inverse Laplace transform. Since the inverse Laplace transform of the MGF could not be found in closed form, an efficient numerical technique is used, which by itself is quite computationally intensive owing to the number of iterations required [33]. On the other hand, the expressions presented in this chapter involve a few evaluations of the exponential function and evaluation of polynomial functions with powers on the order of the number of antennas on a node. The authors in [34] derived exact outage probability of the output SINR for an LMMSE receiver with interferers having arbitrary average powers in a flat Rayleigh fading channel. The expression obtained therein involves the determinant of a  $M \times M$  matrix ( $M$  being the number of receive antennas) and each of its elements involve computation of an incomplete Gamma function. However, [34] has a different system model because the chapter treats both transmit and receive beamforming.

There are other works that provide bounds and approximations to these quantities. The authors in [40] derived an upper bound on the symbol error probability (SEP) of the LMMSE receiver for equal-power co-channel interferers in an uncorrelated Rayleigh fading environment. Another work [41] derived closed form approximations for the LMMSE receiver with two receiver antennas and arbitrary number of interferers. [22] also considers only equal-power interferers and uncorrelated received signals. Even with the simplifying approximation it needs numerical integration. A semi-analytical approach was proposed in [52] for obtaining an approximate expression for the SINR cumulative distribution function (CDF) and ABER for LMMSE receiver. It requires Monte Carlo computation of the average eigenvalues (EVs) of

the interference covariance matrix; this is the part that makes the expression semi-analytical.

Once the analytical expressions of the SINR distribution and the ABER for LMMSE receiver are derived using the approximate average eigenvalues, they are used to develop collision models for LMMSE MMSE-DF receivers. These analytical collision models are derived only for two antenna receivers with arbitrary number of equal powered interfering users or arbitrary number of receive antennas and three interferers with different powers. For other scenarios the semi-analytical expressions in [52] are used.

The rest of the chapter is organized as follows. The system model when using the LMMSE receiver is presented in Section 3.2. This section also presents the expressions of the SINR PDF, CDF, and ABER derived in [52]. These expressions are a function of the average eigenvalues of the noise-plus-interference covariance matrix that was obtained using monte carlo simulations in [52]. In Section 3.3 exact and approximate expressions of these average eigenvalues are derived. Based on the expressions in sections 3.2 and 3.3 SINR- and ABER-based collision models are developed in section 3.4. Finally, the chapter is summarized in 3.5.

## ***3.2 Performance Analysis of LMMSE Receiver***

We consider a MIMO system with  $M$  antennas at the receiver, and a total of 3 single-antenna transmitters. In practical applications, such a receiver can be a BS in cellular, and access point in an infrastructure wireless LAN, or a node in an ad hoc network. The  $M$ -antenna receiver can be a base station, an access-point, or a receiver node in ad-hoc network as mentioned above. The  $M \times 1$  received signal at the array is

$$\mathbf{x} = \sum_{i=0}^L \sqrt{a_i} \mathbf{v}_i s_i^H + \mathbf{n}, \quad (12)$$

where  $\sqrt{a_i}$  is the received signal amplitude representing path loss and  $\mathbf{v}_i$  is a vector of independent unit variance complex normal random variables representing the flat Rayleigh fading channel,  $s_i$  is the transmitted symbol of the  $i^{\text{th}}$  user, and  $\mathbf{n}$  is the receiver noise. The desired user is indexed 0. The post processor SINR of the optimum LMMSE combiner [52] is given by

$$\gamma = a_0 \mathbf{v}_0^H \mathbf{\Phi}^{-1} \mathbf{v}_0, \quad (13)$$

where  $\mathbf{\Phi}$  is the interference-plus-noise covariance matrix. Assuming uncorrelated noise and interference and quasi-static flat fading such that the gain remains constant over the whole packet, we have

$$\mathbf{\Phi} = \sigma^2 \mathbf{I} + \sum_{i=1}^L a_i \mathbf{v}_i \mathbf{v}_i^H, \quad (14)$$

where  $\mathbf{I}$  is the identity matrix and we assume that all branches have same noise power  $\sigma^2$ .

The CDF and PDF of the post LMMSE processing SINR used in this thesis were originally developed by Pham and Balmain in [52]. Parts of their derivation have been reproduced in the following for ease of reading this thesis. The derivation of the CDF of output SINR [52] uses the fact that propagation vectors are complex multivariate Gaussian variables that have distribution

$$p_j(\mathbf{u}_j) = \frac{1}{\pi^M |R_j|} \exp(-\mathbf{u}_j^H R_j^{-1} \mathbf{u}_j), \quad 0 \leq j \leq L \quad (15)$$

where  $||$  denotes determinant and  $\mathbf{u}_j = \sqrt{a_j} \mathbf{v}_j$ . Since all signals are assumed to have independent fading, the joint density function of  $\mathbf{u}_0, \mathbf{u}_1, \dots, \mathbf{u}_L$  is given by

$$p_u(\mathbf{u}_0, \mathbf{u}_1, \dots, \mathbf{u}_L) = \prod_{j=0}^L p_j(\mathbf{u}_j). \quad (16)$$

The PDF of the output SINR [52] can be found by first determining the characteristic function through the Laplace transform

$$\Psi(z) = \int_0^\infty p(\gamma) \exp(-z\gamma) d\gamma. \quad (17)$$

After evaluation of (17) the characteristic function is an expectation of  $G(z, \lambda_1, \dots, \lambda_M)$  with respect to  $\lambda_1, \dots, \lambda_M$ , where  $\lambda_i$ 's are the eigenvalues of  $\Phi \mathbf{R}_0^{-1}$  and

$$G(z, \lambda_1, \dots, \lambda_M) = \prod_{i=1}^M \frac{\lambda_i}{z + \lambda_i} \quad (18)$$

The expectation is computed by approximating  $\Psi(z)$  using Taylor series expansion and retaining only the first order moment terms. Thus

$$\Psi(z) \approx \prod_{i=1}^M \frac{E[\lambda_i]}{z + E[\lambda_i]} \quad (19)$$

The PDF of the output SINR can now be determined by an inverse Laplace transform of  $\Psi(z)$ . By using a partial fraction expansion  $\Psi(z)$  can be written as a sum of simple fractions whose inverse Laplace transforms are known. The mean eigenvalues appearing in (19) are all real and positive due to the positive definite and Hermitian nature of  $\Phi$  and  $\mathbf{R}_0$ . If the number of interferers,  $L$ , is less than the number of antennas then there are  $L (< M)$  mean eigenvalues of multiplicity one and one mean eigenvalue of multiplicity  $M - L$ . Using partial fraction expansion (PFE) (19) can be written in the form

$$\Psi(z) \approx \sum_{i=1}^L \frac{B_i}{z + E[\lambda_i]} + \sum_{i=1}^{M-L} \frac{C_i}{(z + E[\lambda_M])^i}, \quad (20)$$

where  $B_i$  and  $C_i$  are coefficients obtained by PFE of (19). Using (20) PDF of the output SINR is found to be

$$\begin{aligned} p(\gamma) &= \mathcal{L}^{-1}(\Psi(z)) \\ &= \sum_{i=1}^L B_i \exp(-E[\lambda_i]\gamma) + \sum_{i=1}^{M-L} C_i \frac{\gamma^{i-1}}{(i-1)!} \exp(E[\lambda_M]\gamma). \end{aligned} \quad (21)$$

Hence, CDF of the output SINR is

$$\begin{aligned} P(\gamma) &= \int_0^\gamma p(\zeta) d\zeta \\ &= \sum_{i=1}^L \frac{B_i}{E[\lambda_i]} [1 - \exp(-E[\lambda_i]\gamma)] \\ &\quad + \sum_{i=1}^{M-L} \frac{C_i}{E[\lambda_M]^i} \left[ 1 - \sum_{k=0}^{i-1} \frac{\gamma^k E[\lambda_M]^k}{k!} \exp(-E[\lambda_M]\gamma) \right]. \end{aligned} \quad (22)$$

The average bit error rate for coherent detection of phase-shift keying (PSK) signals is given by

$$\begin{aligned}
ABER &= \int_0^\infty p(\gamma) \operatorname{erfc}(\sqrt{\gamma}) d\gamma \\
&= \sum_{i=1}^N B_i \left( \frac{\sqrt{1 + E[\lambda_i]} - 1}{2E[\lambda_i]\sqrt{1 + E[\lambda_i]}} \right) + \sum_{i=0}^{M-L} C_i \left( \frac{\sqrt{1 + E[\lambda_M]} - 1}{2E[\lambda_M]\sqrt{1 + E[\lambda_M]}} \right)^i \\
&\quad \sum_{k=0}^{i-1} \binom{i-1+k}{k} \left( \frac{\sqrt{1 + E[\lambda_M]} - 1}{2\sqrt{1 + E[\lambda_M]}} \right)^k
\end{aligned} \tag{23}$$

As can be seen from (21), (22), and (23), the post processing SINR PDF and CDF and ABER are a function of the average eigenvalues of noise plus interference covariance matrix. The authors in [52] used Monte Carlo simulations to compute these values. Exact and average closed form expressions of the approximate average eigenvalues is computed in the following section. It will be seen later that using the average values derived in the following section gives fairly accurate ABER and distribution of SINR.

### 3.3 Average Eigenvalue(s) of a Random Matrix

In this section, we will derive exact and approximate expressions for the average EVs of a random matrix. The approximate expressions, as will be shown later, have a very simple form that can be easily used for SINR- or BER-based performance analysis using LMMSE receivers.

Consider a random matrix given by

$$\Phi_I = \sum_{i=1}^L a_i \mathbf{v}_i \mathbf{v}_i^H = \mathbf{V} \mathbf{A} \mathbf{V}^H, \tag{24}$$

where  $\mathbf{V} = [\mathbf{v}_1, \mathbf{v}_2 \cdots \mathbf{v}_L]^T$  is a  $M \times L$  matrix,  $\mathbf{v}_i \sim CN(\mathbf{0}, \mathbf{I}_M)$  is a  $M \times 1$  complex random vector, and  $\mathbf{A} = \operatorname{diag}(a_1, a_2 \cdots a_L)$  such that  $a_i, i = 1, 2, \dots, L$  are deterministic values. In our application,  $M$  is the number of receiver antennas and  $L$  is the number of independent interference data streams falling on the receive array. We will primarily consider the matrix  $\Phi_I$  for  $L = 2$  and with  $M \geq L$ ; however, the results

will also hold for  $M = 2$  and  $M < L$  (overloaded case) when the interferers are equal powered. This is true because the SINR CDF is a function of average eigenvalues of  $\Phi_I$ . In the overloaded case, when the interferers are equal powered, the non-zero eigenvalues of  $\tilde{\Phi}_I = a\mathbf{V}^H\mathbf{V}$  are the same as those of  $\Phi_I$ , where  $a = a_i \forall i$ . It should be noted that the above notation has been abused to establish the duality.

The following is the derivation for the approximate largest average EV. Using some well known properties of the trace (Tr) operator [66],

$$\sum_{i=1}^L \lambda_i = \text{Tr}(\Phi_I) = \text{Tr}(\sum_{i=1}^L a_i \mathbf{v}_i \mathbf{v}_i^H) = \sum_{i=1}^L a_i \text{Tr}(\mathbf{v}_i \mathbf{v}_i^H). \quad (25)$$

Taking the expectation of both sides and interchanging  $E[\cdot]$  and  $\text{Tr}(\cdot)$  using the linear nature of the two operators we obtain

$$\sum_{i=1}^L E[\lambda_i] = \sum_{i=1}^L a_i \text{Tr}(E[\mathbf{v}_i \mathbf{v}_i^H]). \quad (26)$$

The argument of the trace operator is the covariance matrix of  $\mathbf{v}_i$ , hence

$$\sum_{i=1}^L E[\lambda_i] = \sum_{i=1}^L a_i \text{Tr}(\mathbf{I}_M) = M \sum_{i=1}^L a_i, \quad (27)$$

where  $\mathbf{I}_M$  is an  $M \times M$  identity matrix. To obtain the approximate asymptotic average of the largest EV, we assume  $a_1 \gg a_i, i \neq 1$ . Hence, we ignore the contribution of weaker EVs and we obtain our approximation for the first average eigenvalue as

$$\widehat{E[\lambda_1]} = M \sum_{i=1}^L a_i. \quad (28)$$

For completeness we bring to the reader's attention that in the trivial but important case of  $L = 1$ , the spectrum of  $\Phi_I$  has only one non-zero EV and it is equal to  $Ma_1$ .

Next, we obtain the average value of the smaller EVs, using the joint PDF of ordered EVs. Computing average EVs for general  $M$  and  $L$  becomes very complicated; hence, we consider only the case of two interfering users ( $L = 2$ ). The joint EV distribution for this case is given by [42], [46], and [72]

$$p_\Lambda(\lambda_1, \lambda_2) = K(\lambda_1 \lambda_2)^{M-2} (\lambda_1 - \lambda_2) \times \left[ \exp\left(-\frac{\lambda_1}{a_1} - \frac{\lambda_2}{a_2}\right) - \exp\left(-\frac{\lambda_1}{a_2} - \frac{\lambda_2}{a_1}\right) \right], \quad (29)$$

where  $K^{-1} = a_1 a_2 (a_1 - a_2)^{M-1} (M-1)! (M-2)!$ . From this, we compute the marginal distribution of  $\lambda_2$  and then the average of the second EV. General expressions for the marginal distribution and the expected value for the smaller EV,  $\lambda_2$ , are derived in the Appendix 3.6. However, this is a complicated expression and it is hard to obtain any insight into the variation of  $E[\lambda_2]$  as a function of interferer powers. Hence, we consider  $M = 2, 3$ , and 4 to gain some insights into our problem.

If  $M = 2$ , the marginal distribution of simplifies to

$$p(\lambda_2) = K_2 (a_1^2 - a_2^2) \exp\left\{-\frac{\lambda_2}{\beta}\right\} \quad (30)$$

where  $K_2 = (a_1 a_2 (a_1 - a_2))^{-1}$  and  $\beta^{-1} = a_1^{-1} + a_2^{-1}$ . Now computing the average  $E[\lambda_2]$ , we obtain

$$E[\lambda_2] = \beta. \quad (31)$$

Now we consider the two interferers ( $L = 2$ ) and three antenna ( $M = 3$ ) scenario. Substituting ( $M = 3$ ) in (62) we obtain the average for this case as

$$E[\lambda_2] = 2(\beta + 2(a_1 a_2)^{-1} \beta^3). \quad (32)$$

(32) is a symmetric relation between  $a_1$  and  $a_2$ , so under high power disparity between the interferers we get the approximate average EV as

$$\widehat{E[\lambda_2]} = 2\beta. \quad (33)$$

The average second EV for two interferers ( $L = 2$ ) and four antennas ( $M = 4$ ) scenario can be obtained following the same procedure as last two cases. It is found to be

$$E[\lambda_2] = 3\left(\beta + \frac{14}{3}(a_1 a_2)^{-1} \beta^3 + 6(a_1 a_2)^{-2} \beta^5\right). \quad (34)$$

We observe that (34) is also a symmetric function of  $a_1$  and  $a_2$ .

We recall our assumption that the eigenvalues of  $\Phi_I$  are distinct. This assumption will be violated when the interferers are separated in space with approximately the

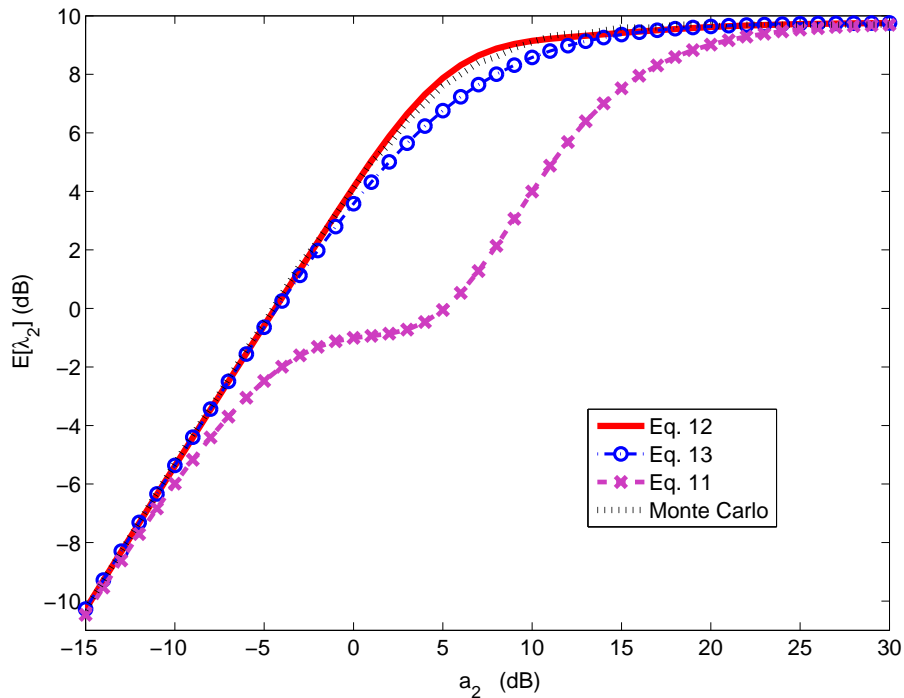


**Figure 4:** Average eigenvalues for  $a_1 = 5$  dB using different computation methods,  $L = 2$  and  $M = 4$

same power. To gain insight into this, we estimated  $E[\lambda_2]$  as a function of  $a_1/a_2$  using Monte Carlo techniques, and modified (34) to get a better fit when  $a_1/a_2 \approx 1$ . The result of that fit is

$$E[\lambda_2] = 3 \left( \beta + \frac{1}{3} (a_1 a_2)^{-1} \beta^3 + 6 (a_1 a_2)^{-2} \beta^5 \right). \quad (35)$$

We observe that the coefficient of the second term in (35) is much reduced compared to (34). This and noting a trend in the three scenarios, we propose the approximation

$$\widehat{E}[\lambda_2] = (M - 1)\beta. \quad (36)$$

The exact expression in (34), the two approximations in (35) and (36), and the Monte Carlo result are shown in Fig. 4. (34) has a large deviation from the Monte Carlo case around 0 dB, because of our assumption. In contrast the simple expression in (36) is very close to the Monte Carlo result, indicating that it mostly overcomes the penalty of the assumption.

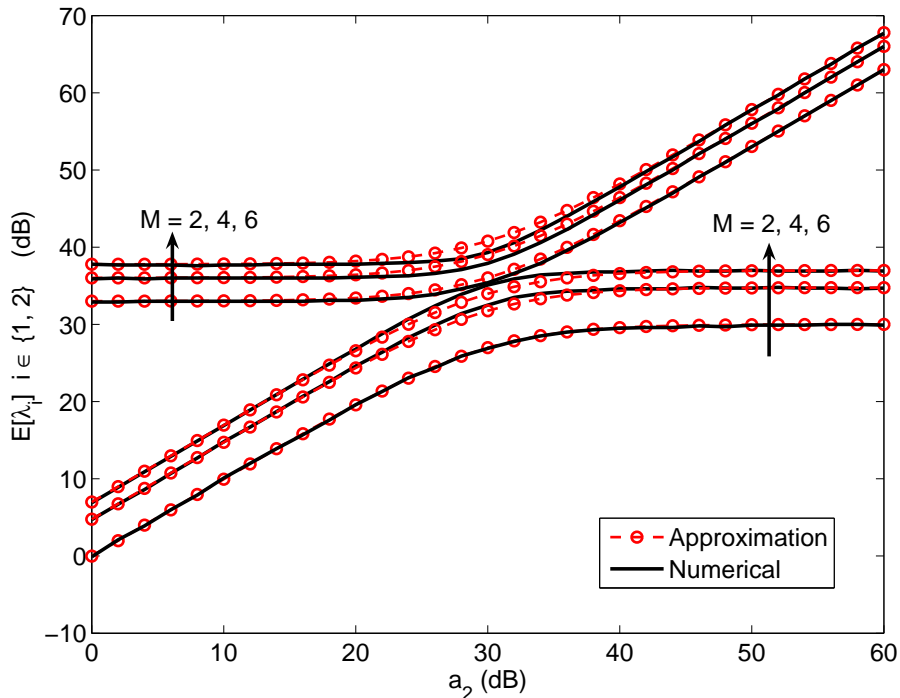


**Figure 5:** Average eigenvalues for  $a_1 = 30\text{dB}$ ,  $L = 2$  and  $M = 2, 4, 6$  using approximate CFE and Monte Carlo simulations

Fig. 5 shows the average EVs computed using Monte Carlo simulation for 2000 channel trials,  $E[\lambda_i]_{mc}, i \in \{1, 2\}$ , and those using the approximations given by (28), and (36). The EVs are computed for  $M = 2, 4$ , and 6. The solid lines show the Monte Carlo computed EVs and the dashed lines with circles are those obtained using the approximation. The horizontal axis is power of one of the interferers,  $a_2$ , in dB and the other interferer has strength of 30 dB. We observe that the approximation is very close for highly disparate interferer powers. The maximum difference occurs when interferers are equal-powered.

Since in Fig. 5 one of the interferers has fixed power it is important to understand what happens to the approximation error when the two interferers have arbitrary power difference. Let  $R = a_1/a_2$ . It is easily shown that  $\beta = R/(R+1)a_2$ . By substituting this into the exact and approximate expressions,  $E[\lambda_i]$  and  $\widehat{E}[\lambda_i]$ , respectively, we were able to show that  $E[\lambda_i]/\widehat{E}[\lambda_i]$  depends only on  $R$ , for  $i = 1, 2$  and  $M = 2, 3$

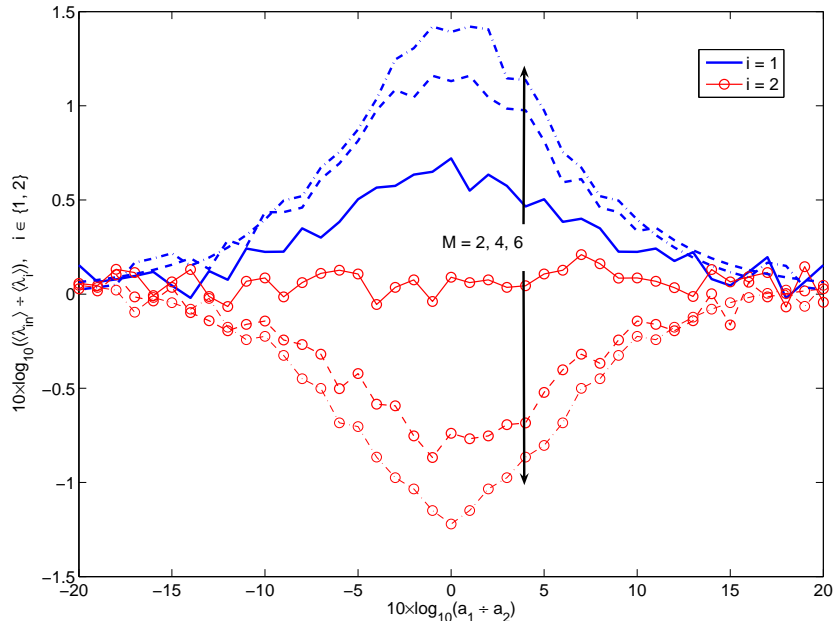


**Figure 6:** Error (in dB) between the approximation and the values obtained using Monte Carlo simulation, of the eigenvalue for  $L = 2$ ,  $M = 2, 4$ , and  $6$

and 4. An exhaustive proof for all  $M$  was not attempted. In Fig. 6, this ratio of true average, obtained by Monte Carlo method, to approximate eigenvalues is plotted in dB versus the interference power ratio  $a_1/a_2$  and for different number of antennas,  $M = 2, 4$ , and  $6$ . We observe that the maximum error grows with  $M$ , but there is less than 1.5 dB difference in the worst case.

Now, we present the SINR and ABER results of LMMSE receiver using the derived CFE with approximate average EVs. These results are compared with the semi-analytical approach in [52]. It was mentioned earlier that the approximate average EVs differ most from the Monte Carlo computed values when interferer powers are equal. Hence, we use the scenario with equal-power interferers for the comparison. It should be noted that the results will be more accurate if interference with different powers are used.

Fig. 8 shows the no-capture probability given by  $Pr\{SINR < \gamma_{th}\}$  with two interferers and one desired user. All the three users have equal average SNR at the

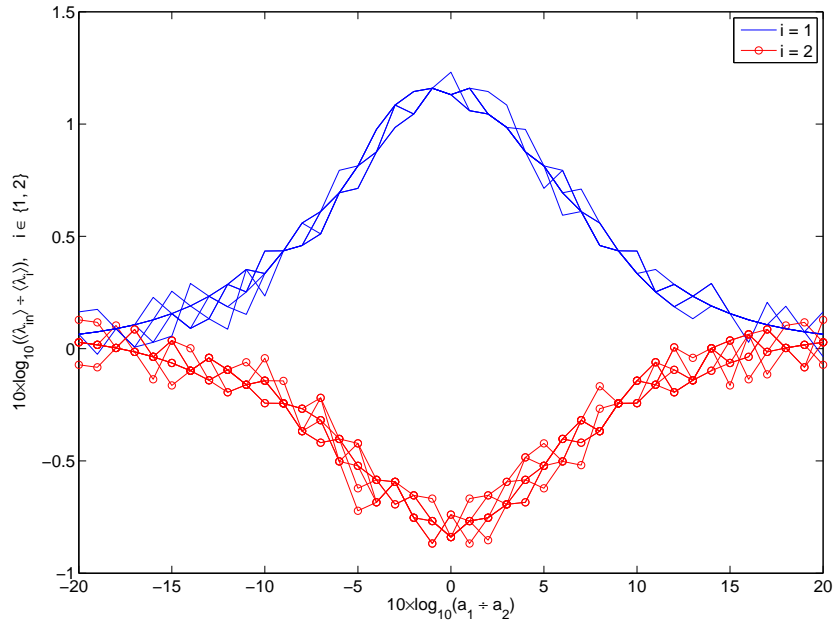


**Figure 7:** Error (in dB) between the approximation and the Monte Carlo simulation values of the eigenvalue for  $L = 2$ ,  $M = 4$ , and parameterized on  $10 \times \log(a_1 a_2)$

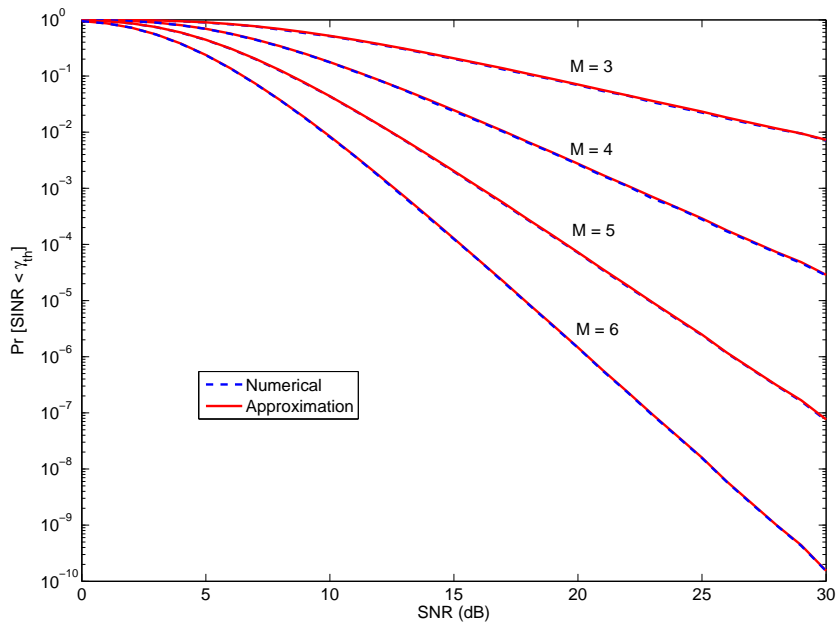


**Figure 8:** No-capture probability with desired user and two interferers having the same SNR and the threshold,  $\gamma_{th} = 9.12$  dB

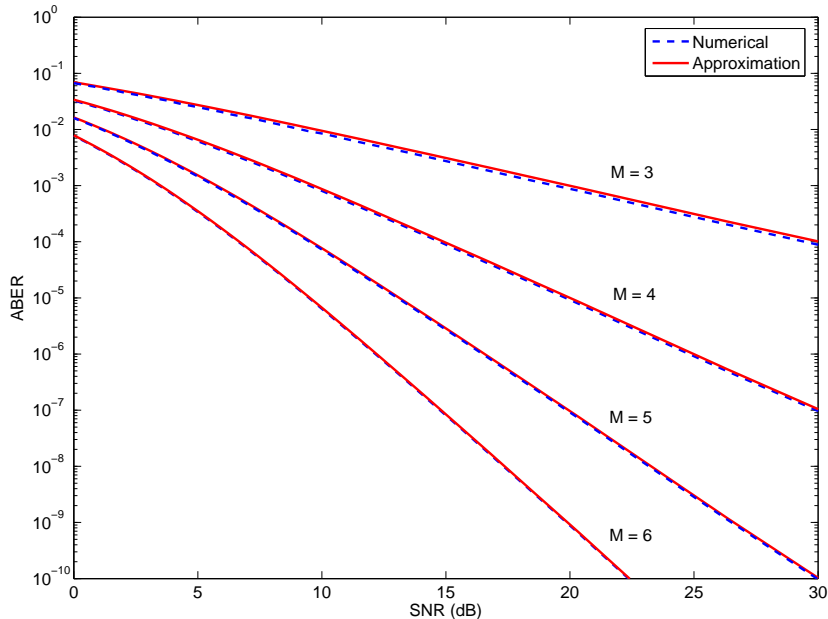


**Figure 9:** ABER for LMMSE receiver using Pham’s approach [52] and the proposed CFE

receiver. The horizontal axis gives the signal-to-noise ratio (SNR) per antenna in dB.  $\gamma_{th}$  is 9.12 dB, which is the SNR required for BER of  $10^{-6}$  using BPSK modulation in an AWGN channel. The probabilities obtained using the Monte Carlo computed EVs are plotted with dashed lines and those obtained using the approximation with solid lines. The curves are parameterized on the number of receiver antennas ( $M = 3, 4, 5,$  and  $6$ ). We observe that the SINR CFE obtained using the approximation is almost the same as the semi-analytical approach.

Fig. 9 shows ABER curves for LMMSE receivers with different numbers of receive antennas ( $M = 3, 4, 5,$  and  $6$ ) and same interference scenario as that in Fig. 7. The modulation is assumed to be BPSK and the channel is flat Rayleigh faded. The horizontal axis gives the range of signal-to-noise ratio (SNR) in dB and the vertical axis represents ABER. The dashed ABER curves are obtained using Monte Carlo average EVs and the solid curves were obtained using the approximate average EVs. ABER is also very close for the two methods.

So far, the accuracy of the CDF and PDF of post LMMSE-processing SINR has been established when using the approximate average eigenvalues of the spatial covariance matrix. The next goal is to develop SINR- and ABER-based collision models of an LMMSE and SIC receiver using equations (22) and (23).

## 3.4 Collision models

In this section different collision models of LMMSE and SIC are derived that can be used for physical layer abstraction in network simulations. These collision models are also used in the thesis to develop analytical/simulation models of random access and ad hoc networks.

### 3.4.1 SINR-based collision models

#### 3.4.1.1 Semi-analytical model

A SISO collision or multi-packet reception model was proposed [56], where it was stated that the capture probability,  $P_{cap}$ , which is the probability that a packet will be correctly decoded if its SINR is greater than a preset threshold,  $\gamma_{th}$  is:

$$P_{cap} = Pr(SINR \geq \gamma_{th}), \quad (37)$$

$P_{cap}$  depends upon the coding and modulation. However, [56] considered only path-loss-dependent received signal strength. Later, a detailed study of capture probability, in presence of multipath, shadowing and the near-far effect was done in [81]. The SINR-based CM is the most popular CM to be used in the network level analytical models. We will extend this model to LMMSE and SIC receivers.

We consider a MIMO system with  $M$  and  $N$  antennas at the receiver and transmitter respectively and a total of  $L + 1$  transmitters. The capture probability is computed as per (22). The required average eigenvalues are computed using Monte Carlo simulations. This makes collision model under discussion a semi-analytical one.

When a MMSE decision feedback (MMSE-DF) MUD receiver is considered, perfect cancelation is assumed at each feedback stage. Hence, the first stage of MMSE-DF has maximum number of interfering users and the following stages have one less interferer compared to the previous stage as discussed in Section 2.1.1. Hence, when there are  $k$  interfering users the capture probability is given as

$$P_{cap}^{MUD} = \prod_{i=1}^k P_{cap}^i, \quad (38)$$

where  $P_{cap}$  is computed as per (37).

#### 3.4.1.2 Analytical model

In this section analytical collision models are derived for two antenna receivers with arbitrary number of equal powered interfering users. In this case, using (28) and (36), the approximate expressions for the average eigenvalues of the interference covariance matrix for an  $M$  antenna receiver is given as

$$\begin{aligned} \bar{\alpha}_1 &= M(P_1 + P_2) \\ \bar{\alpha}_2 &= (M - 1)\left(\frac{1}{P_1} + \frac{1}{P_2}\right)^{-1}, \end{aligned} \quad (39)$$

where  $P_i$  is the received power of the  $i$ -th user. If received power from both the users is the same,  $p = P_1 = P_2$ , then the approximation becomes

$$\bar{\alpha}_1 = 2MP \quad \text{and} \quad \bar{\alpha}_2 = (M - 1)\frac{P}{2}. \quad (40)$$

To use the above result in an S-ALOHA framework with more than two users in the network, we need to generalize it for an arbitrary number of users. We use the theorem that non-zero eigenvalues of  $\mathbf{H}\mathbf{H}^H$  and  $\mathbf{H}^H\mathbf{H}$ , where  $\mathbf{H}$  is an  $M \times L$  matrix are the same [66]. Hence, eigenvalues of interference covariance matrix for two antennas with  $M$  users is the same as those for  $M$  antennas and two users. This allows us to use the SINR CDF developed earlier in this chapter in the framework of

S-ALOHA network. The expression for SINR CDF can be obtained using (22)

$$P(\gamma) = Pr(SINR \leq \gamma) = \sum_{i=1}^M \frac{B_i}{\lambda_i} [1 - \exp(-\bar{\lambda}_i \gamma)]. \quad (41)$$

For all equal power interferers and the desired user case, (41) can be re-written using the average eigenvalue approximations in (40) as

$$P(\gamma|M, \bar{\gamma}) = 1 - \frac{\bar{\lambda}_1 \bar{\lambda}_2}{\bar{\lambda}_1 - \bar{\lambda}_2} \left[ \frac{e^{-\bar{\lambda}_2 \gamma}}{\bar{\lambda}_2} - \frac{e^{-\bar{\lambda}_1 \gamma}}{\bar{\lambda}_1} \right] \quad (42)$$

The probability of no-capture for SINR based CM can now be obtained by setting a SINR threshold,  $\gamma_{th}$ :

$$P(\gamma_{th}|M, \bar{\gamma}) = 1 - \frac{\bar{\lambda}_1 \bar{\lambda}_2}{\bar{\lambda}_1 - \bar{\lambda}_2} \left[ \frac{e^{-\bar{\lambda}_2 \gamma_{th}}}{\bar{\lambda}_2} - \frac{e^{-\bar{\lambda}_1 \gamma_{th}}}{\bar{\lambda}_1} \right]. \quad (43)$$

### 3.4.2 ABER-based collision models

In this section we derive the ABER based collision model that is not only closer to providing a more realistic PHY layer abstraction but also allows a detailed analysis of the network performance for different PHY parameters. In this thesis, we consider the following parameters: packet length, error control coding, and modulation.

A Gaussian approximation on the interferers is used to simplify the BER collision model. Let  $P_b(\gamma)$  be the BER when the interferers are approximated to be Gaussian and the equivalent SINR is  $\gamma$ . If the packet length is  $L$  then the probability that the packet is successfully received for the specified SINR is

$$P_s(L, \gamma) = (1 - P_b(\gamma))^L. \quad (44)$$

A flat, block fading channel is assumed such that all the bits in the packet undergo the same amount of fading. Hence, the probability of capture for a packet with an average SINR,  $\bar{\gamma}$ , is then

$$P_{NC}^{ABER}(M, \bar{\gamma}, L) = 1 - \int_0^{\infty} P_s(L, \gamma) p(\gamma|M, \bar{\gamma}) d\gamma, \quad (45)$$

where,  $p(\gamma|M, \bar{\gamma})$  is the SINR probability density function for an LMMSE receiver that is obtained by differentiating (42) w.r.t  $\gamma$ . It can be observed from (44) and (45) that the capture probability obtained using the BER collision model depends upon  $L$  and  $P_b(\gamma)$ . The latter is a function of the type of modulation; hence, to model the effect of modulation we need to plug-in the appropriate expression of the BER.

A closed form solution of (45) is difficult to obtain and numerical computation results in inaccuracy at high SNR values because of the very low  $P_b(\gamma)$  values involved. Hence, we separate the integration into two with different limits. The first integral, given in (46), will be computed numerically as.

$$P_C^1(M, \bar{\gamma}) = \int_0^{\gamma_0} P_s(L, \gamma) p(\gamma|M, \bar{\gamma}) d\gamma. \quad (46)$$

The second uses two approximations: (i)  $P_s(L, \gamma) = 1 - LP_b(\gamma)$  at high SNRs and (ii) given in (47)

$$Q(x) = \frac{1}{x\sqrt{2\pi}} \exp\left(-\frac{x^2}{2}\right). \quad (47)$$

The second approximation helps in obtaining a simple closed form expression for the second integral, given in (48), without much loss in accuracy. Using approximation (i) we get the second integral as

$$P_C^2(M, \bar{\gamma}) = \int_{\gamma_0}^{\infty} (1 - LP_b(\gamma)) p(\gamma|M, \bar{\gamma}) d\gamma. \quad (48)$$

The closed form solution of (48) is derived in the Appendix 3.7. To model different modulations  $P_b(\gamma)$  should be selected accordingly [15] (pg 217). Using (46) and (48) the ABER based CM can now be written as

$$P_{NC}^{ABER}(M, \bar{\gamma}) = 1 - P_C^1 - P_C^2. \quad (49)$$

Coding can be used to improve the probability of capture for a packet. The BCH codes are examined to determine the effects of coding in presence of interfering packets. For a given probability of bit error, the probability of survival of a packet of

length  $L$  is given by

$$P_p(n|\gamma) = \sum_{i=0}^t \binom{L}{i} (1 - P_b(n|\gamma))^{L-i} (P_b(n|\gamma))^i, \quad (50)$$

where,  $t$  is the number of bits the error correction code can correct. For an un-coded system  $t = 0$  and the equation reduces to (44).

### 3.5 Summary

We have derived very simple CFEs for approximate average EVs of interference covariance matrix for two interferers. The interferers can have different average powers. The CFE for ABER using the approximate average EVs are very close to that obtained using Monte Carlo simulation [52] under the worst case approximation. Further SINR- and ABER-based collision models of LMMSE receiver are developed. SINR-based collision model of MMSE-DF receiver is also developed. These models can be used to capture the effect of multiple antenna physical layer in network level analysis.

### 3.6 Appendix 3.6: Average Eigenvalues of Wishart Matrix

Here we derive the average of the smaller EV of the Wishart random matrix discussed in section II. We begin with the joint pdf, Eq. 29, of the two non-zero EVs. The marginal distribution of  $\lambda_2$  is computed as

$$p(\lambda_2) = \int_{\lambda_2}^{\infty} p(\lambda_1, \lambda_2) d\lambda_1. \quad (51)$$

We break down the integrand into two parts as shown below,

$$p(\lambda_1, \lambda_2) = p_1(\lambda_1, \lambda_2) - p_2(\lambda_1, \lambda_2), \quad (52)$$

where

$$p_1(\lambda_1, \lambda_2) = K f(\lambda_1, \lambda_2) \exp\left(-\frac{\lambda_1}{a_1} - \frac{\lambda_2}{a_2}\right) \quad (53)$$

and

$$p_2(\lambda_1, \lambda_2) = K f(\lambda_1, \lambda_2) \exp\left(-\frac{\lambda_1}{a_2} - \frac{\lambda_2}{a_1}\right), \quad (54)$$

where  $K^{-1} = a_1 a_2 (a_1 - a_2)^{M-1} (M-1)! (M-2)!$  and  $f(\lambda_1, \lambda_2) = (\lambda_1 \lambda_2)^{M-2} (\lambda_1 - \lambda_2)$ .

For notational convenience the arguments of the joint pdfs will be dropped from here on. Now the marginal distribution of  $\lambda_2$  will be computed using  $p_1$  and then use this result for computing  $p_2$  by simply exchanging  $a_1$  and  $a_2$  (Note the symmetry in  $p_1$  and  $p_2$  from Eqs. 53 and 54.)

$$\begin{aligned} p_1(\lambda_2) &= \int_{\lambda_2}^{\infty} p_1(\lambda_1, \lambda_2) d\lambda_1 \\ &= K \int_{\lambda_2}^{\infty} (\lambda_1 \lambda_2)^{M-2} (\lambda_1 - \lambda_2) \exp\left(-\frac{\lambda_1}{a_1} - \frac{\lambda_2}{a_2}\right) d\lambda_1 \\ &= K \lambda_2^{M-2} \exp\left(-\frac{\lambda_2}{a_2}\right) \left[ \int_{\lambda_2}^{\infty} \lambda_1^{M-1} \exp\left(-\frac{\lambda_1}{a_1}\right) d\lambda_1 - \lambda_2 \int_{\lambda_2}^{\infty} \lambda_1^{M-2} \exp\left(-\frac{\lambda_1}{a_1}\right) d\lambda_1 \right] \end{aligned} \quad (55)$$

Using the definition of incomplete Gamma function,

$$\Gamma(n, x) = \int_x^{\infty} t^{n-1} \exp(-t) dt = (n-1)! \exp(-x) \sum_{k=0}^{n-1} \frac{x^k}{k!} = (n-1)! \exp(-x) e_{n-1}(x), \quad (56)$$

into the first integral within the bracket in Eq. 55 we get

$$I_1 = \int_{\lambda_2}^{\infty} \lambda_1^{M-1} \exp\left(-\frac{\lambda_1}{a_1}\right) d\lambda_1 = a_1^M (M-1)! \exp\left(-\frac{\lambda_2}{a_1}\right) e_{M-1}\left(\frac{\lambda_2}{a_1}\right). \quad (57)$$

Similarly, the second integral is computed as

$$I_2 = a_1^{M-1} \lambda_2 (M-2)! \exp\left(-\frac{\lambda_2}{a_1}\right) e_{M-2}\left(\frac{\lambda_2}{a_1}\right). \quad (58)$$

After substituting Eqs. 57 and 58 in Eq. 55 we obtain

$$p_1(\lambda_2) = K \lambda_2^{M-2} \exp\left(-\frac{\lambda_2}{a_2}\right) \left[ a_1 \lambda_2^{M-1} + a_1^{M-1} \times (M-2)! e_{M-2}\left(\frac{\lambda_2}{a_1}\right) (a_1(M-1) - \lambda_2) \right]. \quad (59)$$

Next, we compute the average eigenvalue,  $E[\lambda_2]$ . Again for the sake of brevity we calculate the result only for  $p_1$ , we represent it as  $E[\lambda_2]_1$ . The second part can be obtained by exchanging  $a_1$  and  $a_2$  as discussed earlier. We compute the following integral

$$E[\lambda_2]_1 = \int_0^{\infty} \lambda_2 p_1(\lambda_2) d\lambda_2. \quad (60)$$

After substituting the value of  $p_1(\lambda_2)$  obtained in Eq. 59 and Eq. 56 into Eq. 60 and separating out the sum terms we get

$$\begin{aligned}
E[\lambda_2]_1 &= K a_1 \int_0^\infty \lambda_2^{2M-2} \exp\left(-\frac{\lambda_2}{a_3}\right) d\lambda_2 + \\
&\quad K a_1^{M-1} (M-2)! \int_0^\infty \lambda_2^{M-1} \exp\left(-\frac{\lambda_2}{a_3}\right) \sum_{k=0}^{M-2} \frac{a_1^{-k}}{k!} \lambda_2^k (a_1(M-1) - \lambda_2) d\lambda_2 \\
&= K a_1 a_3^{2M-1} \Gamma(2M-1) + K a_1^M (M-1)! \sum_{k=0}^{M-2} \frac{a_3^{M+k}}{k! a_1^k} \Gamma(M+k) - \\
&\quad K a_1^{M-1} (M-2)! \sum_{k=0}^{M-2} \frac{a_3^{M+k+1}}{k! a_1^k} \Gamma(M+k+1)
\end{aligned} \tag{61}$$

Once we obtain 62, we can compute  $E[\lambda_2]$  as

$$E[\lambda_2] = E[\lambda_2]_1 - E[\lambda_2]_2, \tag{62}$$

where  $E[\lambda_2]_2$  can be obtained by replacing  $a_1$  with  $a_2$ .

### 3.7 Appendix 3.7: Analytical expression of (48)

The intermediate steps of deriving (49) from (48) are given here. Rewriting (48) as

$$P_C^2 = \int_{\gamma_0}^\infty p(\gamma|M, \bar{\gamma}) d\gamma - \int_{\gamma_0}^\infty L P_b(\gamma) p(\gamma|M, \bar{\gamma}) d\gamma = P_C^{21} - P_C^{22}, \tag{63}$$

where,  $P_C^{21}$  and  $P_C^{22}$  are first and second integrals, respectively.  $P_C^{21}$  is the complementary CDF of the SINR evaluated at  $\gamma_0$ , which can be obtained using Eq. 10 as

$$P_C^{21} = 1 - P(\gamma_0|M, \bar{\gamma}). \tag{64}$$

To simplify  $P_C^{22}$  we use the high SNR approximation of the Q-function as given in (47).  $P_b(\gamma)$  can be written in general form as

$$P_b(\gamma) = \alpha Q(\sqrt{\beta\gamma}), \tag{65}$$

with  $\alpha = \beta = 1$  for BPSK/QPSK and  $\alpha = 2(1 - 1/\sqrt{M})$ ,  $\beta = 3/(M-1)$  for M-QAM. After substituting (65) and PDF of SINR, i.e. derivative of (43), we obtain

$$P_C^{22} = K \int_{\gamma_0}^\infty \frac{1}{\sqrt{\gamma}} e^{-\beta\gamma} \left( e^{-\lambda_2\gamma} - e^{-\lambda_1\gamma} \right) d\gamma, \tag{66}$$

where,  $K = L\alpha (2\sqrt{\beta\pi}) \bar{\lambda}_1\bar{\lambda}_2/(\bar{\lambda}_1 - \bar{\lambda}_2)$ . Re-writing (66) as follows

$$P_C^{22} = K \left[ \int_{\gamma_0}^{\infty} \gamma^{\frac{1}{2}-1} e^{-(\beta+\bar{\lambda}_2)\gamma} d\gamma - \int_{\gamma_0}^{\infty} \gamma^{\frac{1}{2}-1} e^{-(\beta+\bar{\lambda}_1)\gamma} d\gamma \right]. \quad (67)$$

We can clearly see that the integrals in (67) are a form of incomplete Gamma function.

Hence, after substituting  $\Gamma(m, \gamma_0) = \int_{\gamma_0}^{\infty} \gamma^{m-1} e^{-\gamma} d\gamma$  into (67), we get

$$P_C^{22} = \frac{K}{\sqrt{\beta + \bar{\lambda}_2}} \Gamma\left(\frac{1}{2}, (\beta + \bar{\lambda}_2)\gamma_0\right) - \frac{K}{\sqrt{\beta + \bar{\lambda}_1}} \Gamma\left(\frac{1}{2}, (\beta + \bar{\lambda}_1)\gamma_0\right). \quad (68)$$

Hence, we obtain the closed form solution of (48) using (63), (65), and (68).

## CHAPTER IV

# RANDOM ACCESS NETWORK - SINGLE CARRIER

### *4.1 Overview*

In the S-Aloha random access channel (RACH), all active terminals are assumed to transmit their (bursty) messages to a single receiver over a common channel in packets of duration  $\tau$ , regardless of the activity of competing terminals. The only network discipline imposed on transmitters is that all transmitted packets must fit into common time slots of length  $\tau$ . (Time slots can be marked in a separate broadcast channel also used to acknowledge reception of successful packets.) An unsuccessful packet will be retransmitted after waiting a random number of slots. The channel is memoryless, i.e. a retransmitted packet experiences collisions uncorrelated with its previous attempts to capture the receiver. Such RACHs have been of interest because of their simplicity since they were first proposed in 1970s [7]. Many existing wireless systems use such channels not only for control signalling [24] and [2] but also for data transfer [5], [57], and [73]. RACH is used for bandwidth request and ranging in the OFDMA-based WiMAX standard [2] and carries short messaging services (SMS) in the WCDMA-based 3GPP standard [5]. As pointed out in the previous chapter there is great interest in using realistic PHY layer models that enable a better analysis of wireless networks. In this chapter, we develop an analytical model of a single carrier narrowband S-Aloha system with LMMSE receiver.

One of the earliest and seminal works used a simple distance based CM [20]. However, the two most common CMs are based on: i) signal to interference ratio (SIR) [9], [22], [13], [78], and [8] and ii) average bit error rate (ABER) [8], [32], [54], and [80]. A number of these models have been developed for the Rayleigh

fading channel. However, most of the models are for omni directional antennas. We presented a novel CM for multiple antenna LMMSE receivers in Chapter III.

Slotted Aloha (S-Aloha) networks have been very frequently used for developing a networking framework. SIR based CMs with Rayleigh fading with a simple path loss model are the most commonly used in such a framework [9], [22], and [13]. Seminal work in [9] and [48] showed that independent fading channel of the interferers result in a higher throughput of S-Aloha network than a line of sight channel (only path loss or distance based collision models). The work in [9] was extended in [13] to include the effect of number of interferers and the choice of modulation. Rician and Nakagami fading with additive white Gaussian noise (AWGN) channels were considered in [78] to compute the throughput. The authors in [8] use both the SIR and ABER based collision models under Nakagami fading. Effect of noise is considered in developing the ABER based CM. This chapter also considers the effect of modulation and packet length on the throughput. More work on ABER based CMs can be found in [32], [54], and [80]. The authors in [54] and [80] introduce the effect of coding along with modulation, packet length and signal to noise ratio (SNR).

In this chapter, we present an analytical model of single carrier slotted Aloha (S-Aloha) network employing a multiple antenna LMMSE receiver. The network model using a general CM is first established. Then SINR- and ABER-based CMs for two antenna LMMSE receiver developed in Chapter III are used in the network model to obtain approximate closed form expressions for the throughput. The analytical model is then used to analyze the effects of coding, modulation, packet length, and SNR. For more than two antenna LMMSE receiver, the SINR outage probability derived in [52] is used.

The rest of chapter is organized as follows. Section 4.2 gives the network model that describes the S-Aloha network and the assumptions therein. Bounds on throughput are also derived in this section. Simulation details and results are presented in

Section 4.3. Finally the chapter is summarized in Section 4.4.

## 4.2 Network Model

We assume that the total number of packets generated in the network (including retransmissions) are Poisson distributed. The validity of this assumption is important when one considers packet delays. This is because if Poisson process for packet generation is assumed, then the assumption that the combined process, of new and retransmitted packets, is Poisson, is valid only when very large packet delays compared to the slot time is allowed [20]. The mean generation rate from each node is  $\lambda$  packets per second. The mean offered channel traffic expressed in packets per time slot is  $G = \lambda\tau$ . The probability of an arbitrary test packet being overlapped by  $n$  other interferers is [20]

$$R_n = \frac{G^n}{n!} e^{-G}. \quad (69)$$

Most of the studies of standard Aloha networks assume that any collision results in a lost packet. It was shown in [9] that Rayleigh fading channel results in improvement in the network throughput. The advent of MIMO technology allows nodes to have multiple antennas. In this thesis we extend the work of [9] to multiple antenna receivers.

The probability of capture by the receiver in an arbitrary time slot is defined as

$$P_{cap} = 1 - \sum_{n=0}^{\infty} R_n P_{NC}^{CM}(n, \bar{\gamma}) \quad (70)$$

where  $P_{NC}^{CM}(n, \bar{\gamma})$  is the probability of no-capture in presence of  $n$  interferers and average SINR  $\bar{\gamma}$ . This probability depends upon the type of CM represented in the superscript. Chapter III discusses these CMs in detail. Using the capture probability of (70) the channel throughput can be stated as

$$S = GP_{cap} \quad (71)$$

The lower bound on the throughput will be obtained when  $P_{NC}^{CM}(n, \bar{\gamma})$  is equal to one. In this case the probability in (70) contains the infinite sum of the terms  $R_n$ . We then recover the classical expression for slotted Aloha

$$S_{min} = Ge^{-G}. \quad (72)$$

However, for any smaller value of  $P_{NC}^{CM}(n, \bar{\gamma})$ , the throughput will exceed (72), as determined by the relative strengths of the packet signals reaching the common receiver, the number of receiver antennas, modulation choice, etc. The upper bound on the throughput is obtained when  $P_{NC}^{CM}(n, \bar{\gamma})$  is equal to zero. In this case the capture probability is one, hence

$$S_{max} = G. \quad (73)$$

This implies that that all the received packets will be captured without any error.

### 4.3 *Simulation and Results*

In this section, we use the SINR- and ABER-based two-antenna analytical CMs given by Eqs. 43 and 49, respectively, in the S-Aloha network model presented in Section 4.2. This model allows us to study the network throughput as a function of different physical layer parameters. The parameters for SINR-based CM (SCM) are: SNR per user and SINR threshold. The parameters for ABER-based CM (ACM) are: modulation, SNR per user, and packet length. In one of the results with SCM, performance of one and two antenna receivers is compared. In all the other results in this section, each node in the network employs a two-antenna receiver.

Fig. 10 shows the throughput,  $S$ , versus mean channel traffic,  $G$ , using SCM in the S-Aloha network with two antenna receiver. Throughput is computed for different received SNRs,  $\bar{\gamma}$  (5 and 30 dB), and SINR thresholds,  $\gamma_{th}$  (2 and 10 dB). We observe that the throughput is about 1.5 times higher when the operating SNR goes up from 5 dB to 30 dB with capture threshold set at 2 dB. Increasing the SNR beyond 30

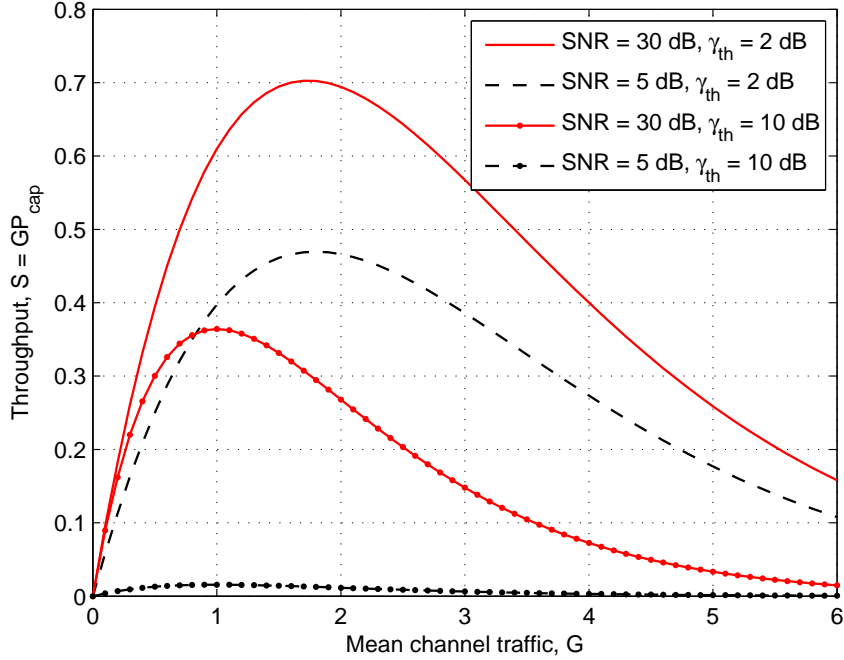


**Figure 10:** Throughput of S-Aloha network employing two antenna LMMSE receiver obtained using SINR-based collision model with different capture thresholds

dB does not result in further increase in throughput. This is because the interferers become dominant beyond this level and hence the effect of noise is reduced. Also, we note that the gain in throughput because of SNR is reduced when we choose a lower  $\gamma_{th}$ . This gain finally reduces to be close to zero when  $\gamma_{th}$  is 10 dB at 5 dB operating SNR. Unlike the maximum throughput of  $1/e$  in the case of conventional S-Aloha without capture. This is because our formulation is a function of SNR, hence, even when there is no interference the capture probability is significantly low when high SNR threshold of 10 dB is set for 5 dB operating SNR. For high operating SNR of 30 dB with 10 dB threshold the performance is very close to conventional S-Aloha with no capture because in this case only interference degrades the performance not the noise.

Next, a comparison in the performance of one- and two-antenna receivers is made in Fig. 11. The capture threshold  $\gamma_{th}$  is 2 dB. The two-antenna scenarios are the

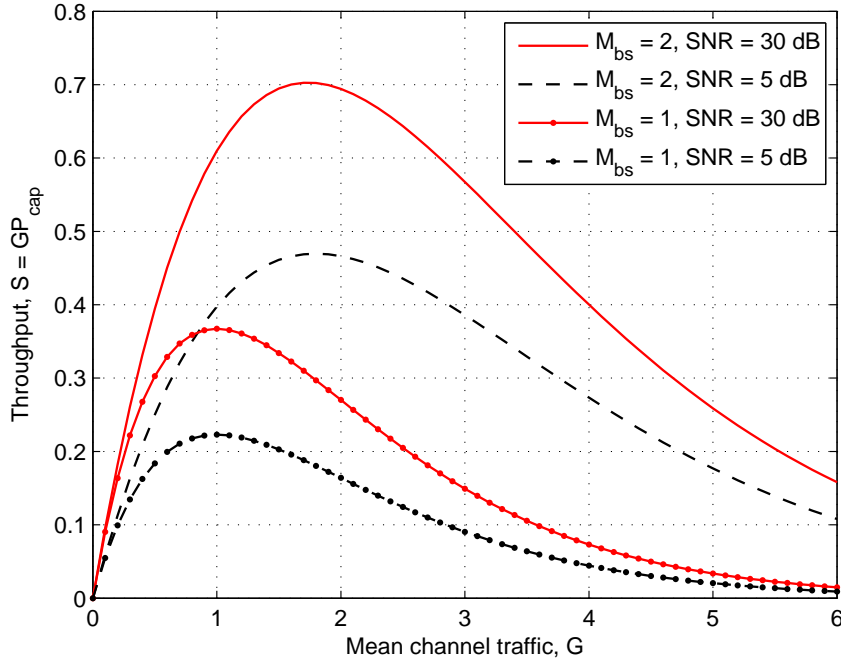


**Figure 11:** Throughput comparison between S-Aloha networks employing either two antenna LMMSE receiver or a single antenna receiver using SINR-based collision model

same as in Fig. 10. In the case of one-antenna receiver, we note that the high SNR performance is same as the conventional S-Aloha without capture because if a packet is received without collision it is successfully received. However, at lower operating SNR the maximum throughput degrades to about 0.22 packets per slot. It is observed that using two antenna receiver almost doubles the maximum throughput, although it is attained at a higher mean traffic rate.

Fig. 12 shows the effect of modulation on throughput using ACM. In particular, BPSK, QPSK, 16-QAM, and 64-QAM constellations are considered. Symbols with different modulations are assumed to have the same time period, such that the bandwidth usage is the same to enable a fair comparison. Also, the slot length is kept constant so that throughput is computed for the mean channel traffic. In order to maintain the same slot length, the number of bits in the packets with higher constellation size is larger. This difference in the number of bits is captured in the collision

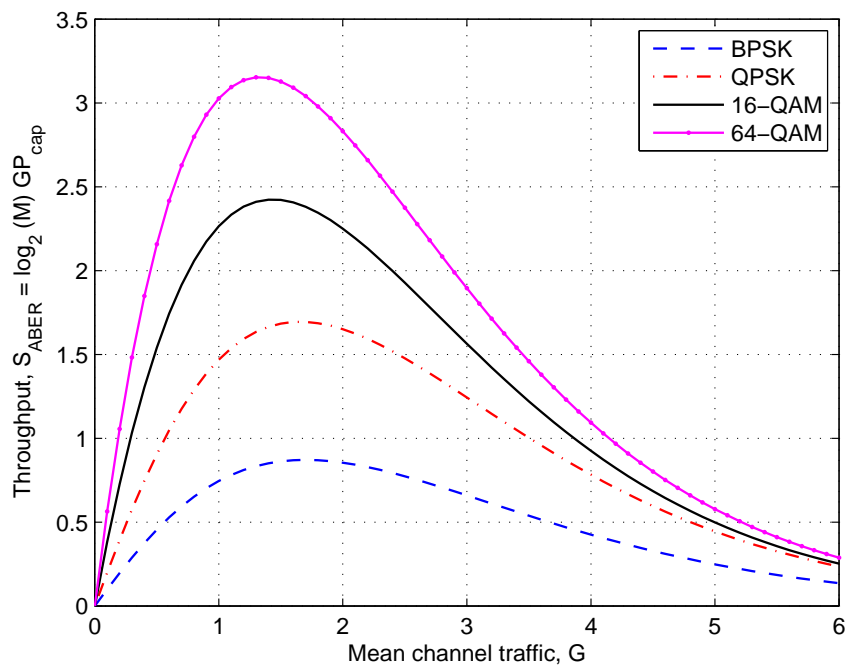


**Figure 12:** Throughput of S-Aloha network, employing two antenna LMMSE receiver, obtained using ABER-based collision model at 20 dB SNR for different modulations and equal packet length.

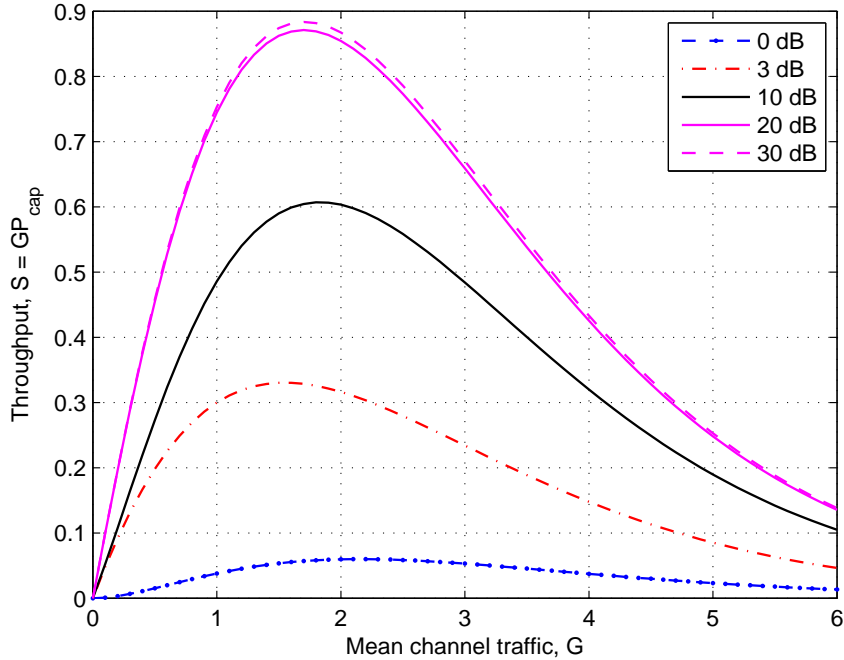


**Figure 13:** ABER-based collision model parameterized on SNR, BPSK modulation,  $L = 128$  bits

model according to Eq. 45. For the simulations in Fig. 12 the packet lengths in terms of number of symbols are  $128 \times \log_2 M$ , where  $M$  is 2, 4, 16, and 64 for BPSK, QPSK, 16-QAM, and 64-QAM, respectively. Since, the total information content in a packet is higher if a larger constellation size is used, hence, the throughput in this case is defined as

$$S_{ABER} = \log_2(M)GP_{cap}, \quad (74)$$

where  $M$  is as defined earlier. The operating SNR is 20 dB for all the users in the network. We observe that the throughput increases by using a higher constellation size. The maximum throughput for the four constellations in order of increasing size is 0.87, 1.69, 2.43, and 3.15. Upon normalizing the maximum throughputs with that of BPSK we obtain the ratio as 1, 1.94, 2.79, and 3.62. It is interesting to note that the throughput does not scale linearly with the information bits. This is because of higher packet error rates associated with larger constellation sizes.

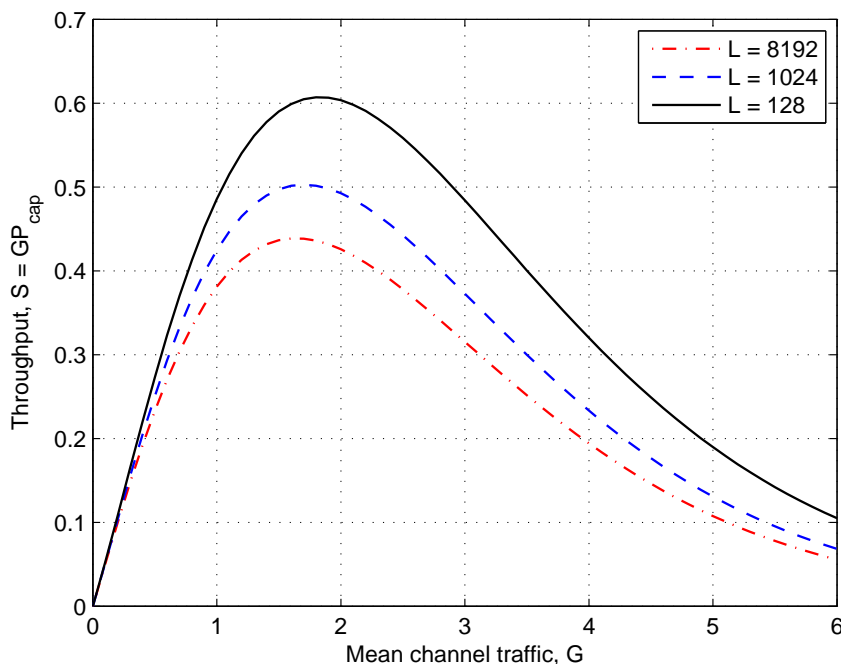


**Figure 14:** ABER collision model without coding, parameterized on packet length for BPSK modulation

Fig. 13 shows the throughput parameterized on SNR (0, 3, 10, 20, and 30 dB). Packets are of length 128 bits and use BPSK modulation. As in Fig. 10 for high capture threshold, the maximum throughput drops below that of conventional S-Aloha, i.e.  $1/e$ . Throughput greater than  $1/e$  is achieved for SNR values greater than 3 dB because of diversity and multiuser detection and saturates for SNR values greater than 20 dB because of interference dominance. Fig. 14 shows the throughput parameterized on packet length (8192, 1024, and 128 bits). The SNR per user is 10 dB and again BPSK modulation is used. We can clearly observe that longer packets result in reduction in throughput because of higher packet error rate.

#### 4.4 Summary

We developed an analytical model for the analysis of single carrier S-Aloha network employing a two antenna LMMSE receiver. Its throughput was compared with that

of a network employing a single antenna receiver using SCM. It was shown that using a single antenna receiver may yield almost zero throughput (in packets per slot) whereas a two antenna receiver yields a throughput of about 0.47 packets per slot for the same configuration. Next, ACM was used to develop a network model and effect of packet length, SNR, and modulation was studied.

# CHAPTER V

## RANDOM ACCESS NETWORK - MULTI-CARRIER

### *5.1 Introduction*

It is well known that S-Aloha systems are unstable when the arrival rates are above a certain threshold. Control mechanisms have been developed to stabilize both single [55] and multichannel [64],[65] S-Aloha networks. Above mentioned schemes require only one-bit feedback per subchannel to the subscriber stations, informing them if the subchannels in the previous slot had a collision or not. The subscriber stations update their retransmission probability based on this feedback. The control mechanism proposed in [55], [65] stabilize the network as well as would have been possible with the perfect knowledge of how many nodes transmitted in each slot. Recent work by Bruvold, et al. in [30] uses this concept to propose contention policies that ensure a specified two-class-QoS as well as stability.

The classical S-Aloha systems are based on the assumption that a packet is successfully received only when there is no collision. However, it has been shown that the variation in the wireless channel conditions and advanced receiver processing enable successful packet reception even under collision [30], [77], [58], [27], [28], [45], [79]. This is called the capture effect.

The capture effect has also been used to model multi packet reception (MPR). MPR is achieved by using advanced signal processing. For example, [30] uses multi-user detection (MUD), assuming all the users transmit on common time and frequency resource, in a DS-CDMA framework. Another example is [28] that uses an adaptive array in a narrow band system. Orthogonal preambles are commonly used for MUD

[3, 15]. The WiMAX standard uses orthogonal preambles in a mode called collaborative spatial multiplexing [2] wherein the interfering users transmit data on common sub-carriers but the pilots are on orthogonal sub-carriers. The authors in [45] consider a synchronous random access network where each colliding packet has a unique preamble that is orthogonal to the other preambles.

The purpose of the work in this chapter is to abstract an analytical model of an OFDMA system employing stabilized S-Aloha based RACH and MUD receiver processing. Only a simple abstraction of MUD is used: a signal is considered successfully received when the channels of all interfering signals can be estimated *and* the number of simultaneous transmissions is less the number of BS antennas. Such an abstraction gives the best possible performance using these techniques. The stabilized S-Aloha model is based on the work in [65]. A capture model for single packet reception in a multi-carrier stabilized S-Aloha network is first proposed. This model can be effectively used for both single and multiple antenna base stations. A multi-packet reception model is also proposed for multi-antenna base station. Two frame structures with orthogonal preambles, with designs similar to those in [2] and [45], have been used to allow multiuser detection. Finally, the performance of this system is analyzed in terms of its throughput and delay.

The rest of the chapter is organized as follows. Section 5.2 gives the background of single and multichannel stabilized S-Aloha system and an analytical model for its performance analysis without capture. Performance analysis of stabilized multichannel S-Aloha system with capture is discussed in Section 5.3 followed by its throughput and delay performance in Section 5.4. Finally, the chapter is concluded in Section 5.5.

## 5.2 Background

Pseudo-Bayesian (PB) algorithm was proposed by Rivest in 1987 for single channel S-Aloha to minimize the average packet transmission delay in the network and at the same time maintaining a constant average throughput [55]. It was later extended for multi-channel S-Aloha by Shen and Li [65]. As mentioned earlier the framework of [65] is used in this chapter, it would be useful to briefly discuss the PB algorithm for single and multi-channel systems. The system model presented in this section will be built upon to include capture in the following section.

### 5.2.1 PB Algorithm for Single Channel S-Aloha

The goal of PB algorithm is to minimize the packet delay between the time the packet is given to a station and the time it is successfully transmitted. In this algorithm, the users with new packets in a slot transmit only in the following slot. The user with a packet to transmit will be called an *active user* and the one without any packet will be called an *inactive user*. If there are  $U$  active users at the beginning of a slot then each user transmits a packet with probability

$$p_r = \frac{1}{U}. \quad (75)$$

As can be seen from (75), to know the transmission probability, each user must know the total number of active users in the network. The PB algorithm only requires a binary feedback of collision or no-collision in the slot to estimate the total number of active users. Each active user updates this estimate in slot  $k + 1$  as

$$\begin{aligned} \hat{U}_{k+1} &= \max\{\hat{\lambda}, \hat{U}_k + \hat{\lambda} - 1\}, \quad \text{for idle or success} \\ &= \hat{U}_k + \hat{\lambda} + (e - 2)^{-1}, \quad \text{for collision,} \end{aligned} \quad (76)$$

where  $\hat{\lambda}$  is the estimate of new packet arrival rate. It can also be estimated very accurately using the feedback information [55]. The users in slot  $k + 1$  transmit with

probability

$$p_r(k+1) = \min\left\{1, \frac{1}{\hat{U}_{k+1}}\right\}. \quad (77)$$

Stability can always be achieved when new packet arrival rate is less than  $e^{-1}$ .

### 5.2.2 PB Algorithm for Multi-Channel S-Aloha

The retransmission probability for the single channel case, as given in (77), can be easily extended for multi-channel S-Aloha as [65]

$$p_r(k+1) = \min\left\{1, \frac{N}{\hat{U}_{k+1}}\right\}, \quad (78)$$

where  $N$  is the total number of channels. The update equation for  $\hat{U}_k$  is given as

$$\hat{U}_{k+1} = \max\{\hat{\lambda}, \hat{U}_k + \hat{\lambda} + C(e-2)^{-1} - (M-C)\}, \quad (79)$$

where  $C$  is the number of channels in which collisions occur.

### 5.2.3 Performance Analysis Without Capture

We assume there are  $V$  users. We assume an inactive user has a constant probability  $p_g$  to generate a new packet. An inactive user which has generated a new packet will become an attempting user at the start of the next time slot. Let  $U_k$  denote the number of attempting users at the beginning of time slot  $k$ . Given retransmission probability  $p_r(k)$ , obviously  $U_{k+1}$  only depends on  $U_k$ . Therefore,  $\{U_k, k = 1, 2, \dots\}$  is a Markov chain given  $p_r(k)$ . However,  $p_r(k)$  is determined by the estimate  $\hat{U}_k$  of  $U_k$ . This complicates system performance analysis. To simplify the analysis, we assume the estimate of  $U_k$  is perfect, i.e.  $\hat{U}_k = U_k, \forall k$ . Under this assumption,  $\{U_k, k = 1, 2, \dots\}$  can be modeled with state space  $\{0, 1, \dots, V\}$ . The analysis for this Markov chain can serve as a performance upper bound for practical systems with imperfect estimate of  $U_k$ .

For the ease of reading, this section briefly discusses parts from Shen and Li's paper [65] that are used in this work. The following is the list of variables used in this

chapter. Some of the variables defined earlier are also listed to have a comprehensive list.

$N$	Number of channels
$M$	Maximum number of collisions that allow at least one success
$V$	Total number of users in the finite user scenario
$U_k$	Number of attempting users at the beginning of slot $k$
$D_k$	Number of successful transmissions in slot $k$
$T_k$	Number of transmitting users in slot $k$
$A_k$	Number of inactive users that have new packet arrivals in slot $k$
$p_g$	Probability of new packet generation
$p_r(k)$	Probability of retransmission in slot $k$

### 5.2.3.1 State Transition Probability

We observe that the Markov chain  $\{U_k, k = 1, 2, \dots\}$  is homogeneous, aperiodic, and irreducible. Let  $P_{i,j}$  be the transition probability from state  $i$  to state  $j$ , i.e.  $P_{i,j} = Pr(U_{k+1} = j | U_k = i)$ ,  $0 \leq i, j \leq V$ . Let random variable  $D_k, 0 \leq D_k \leq \min(M, U_k)$  denote the number of successful transmissions at time slot  $k$ . Let  $A_{k+1}, 0 \leq A_{k+1} \leq V - U_k$  be the number of inactive users having new packet generated in time slot  $k$ , which means  $A_{k+1}$  users will become attempting users at slot  $k + 1$ .

The state transition of  $\{U_k, k = 1, 2, \dots\}$  satisfies

$$U_{k+1} = U_k - D_k + A_{k+1}. \quad (80)$$

Given  $D_k = d, U_{k+1} = j, U_k = i$ , we have

$$A_{k+1} = j - i + d. \quad (81)$$

We observe that when there is no attempting user, there is no departure, i.e., when  $i = 0$ , then  $d = 0$ , so that from (81),  $U_{k+1} = A_{k+1}$ . When there is one attempting user, i.e.,  $i = 1$ , under the assumption of perfect user information, there is  $p_r = 1/i = 1$ .

Thus the user will always transmit and be successful. Then  $d = 1$ , and accordingly  $U_{k+1} = A_{k+1}$ . It is easy to get transition probabilities of

$$P_{0,j} = P_{1,j} = \text{bin}(j, V, p_g), \quad (82)$$

where  $\text{bin}(j, V, p_g)$  denotes the binomial probability  $\text{bin}(j, V, p_g) = {}^V C_j p_g^j (1 - p_g)^{V-j}$ .

As can be seen from (78), conditioned on the event of retransmissions,  $U_{k+1}$  only depends upon  $U_k$ . Therefore,  $\{U_k, k = 1, 2, \dots\}$  is a Markov chain given  $p_r(k)$ . The first step is to compute the state transition probabilities  $P_{ij} = Pr\{U_{k+1} = j | U_k = i\}$ ,  $0 \leq i, j \leq V$ . To introduce capture effect into the state transition probabilities,  $Pr\{D_k = d | T_k = t\}$  needs to be modified because  $P_{ij} = \mathcal{F}(Pr\{D_k = d | T_k = t\})$ , where  $D_k$  is bounded as  $0 \leq D_k \leq \min(M, U_k)$ . Details of the derivation of  $\mathcal{F}$  are given in [65]. In this chapter,  $Pr\{D_k = d | T_k = t\}$  is derived to obtain the results for finite user cases with different types of capture.

Asymptotic analysis for the infinite user case is also done in this chapter to obtain the bounds on average network throughput and delay. Our approach to obtain the of the infinite user results is different from that in [65].

### 5.2.3.2 Performance Evaluation

The steady state probability  $\pi = [\pi_1, \pi_2, \dots, \pi_V]$  can be calculated from the transition probability  $\mathbf{P}$  by

$$\begin{aligned} \pi &= \pi \mathbf{P}, \\ \sum_{n=0}^V \pi_n &= 1, \end{aligned} \quad (83)$$

where  $\pi_n = Pr\{U_\infty = n\}$ . The elements of  $\mathbf{P}$  are computed as detailed in [65].

The average number of attempting users is given by

$$\bar{U} = \sum_{n=0}^V n \pi_n \quad (84)$$

The average throughput is

$$\bar{D} = \sum_{n=0}^N n Pr\{D_k = n\}. \quad (85)$$

The probability  $Pr\{D_k = n\}$  can be calculated as

$$\begin{aligned} Pr\{D_k = n\} &= \sum_{i=n}^V Pr\{D_k = n|U_k = i\}Pr\{U_k = i\} \\ &= \sum_{i=n}^V \pi_i Pr\{D_k = n|U_k = i\}, \end{aligned} \quad (86)$$

At the end of a time slot,  $D_k$  users are successful in transmission, and  $B_k = U_k - D_k$  users continue to attempt in the next slot.  $B_k$  is the backlog of slot  $k$ . The average backlog can be computed as

$$\bar{B} = \bar{U} - \bar{D}. \quad (87)$$

### 5.3 Stabilized MC-Aloha with Capture

As mentioned in the previous section, the capture effect can be modeled in different ways depending upon the physical layer characteristics. Three physical layer variants are considered. The first type encompasses single packet reception under collision. The second and the third types model multi-packet reception (MPR). Single packet reception under collision can also be viewed as the capture model where only the packet with  $Pr\{SINR > \gamma_{th}\}$  is received successfully. Such a system may have single antenna or multiple antennas. In the case of MPR, a frame structure consisting of preamble and data is first defined. Two different preamble designs are considered to facilitate MPR. These form the basis of the other two capture models proposed in this chapter. In the following sections  $Pr\{D_k = d|T_k = t\}$  will be calculated for each of the proposed capture models. These capture models will then be used to compute network performance in terms of throughput and delay of stabilized multi-channel S-Aloha network. Performance of the stabilized algorithm with capture is analyzed for both finite and infinite number of users.

### 5.3.1 Single Packet Reception

#### 5.3.1.1 Finite Users

We need to compute the probability of  $d$  successs given  $K$  users transmit in  $N$  channels,  $P(d|K)$ . We assume that only one packet can be successfully received under collision. This occurs when the base station can estimate the channel of only the user whose SINR is maximum. In the general form we get the probability of success as

$$P(d|K) = \binom{N}{d} \sum_{n=d}^{\min(K-d-1, Md)} \binom{K}{n} \times \frac{E_s(d, n)E_f(N - d, K - n)}{N^K} \quad (88)$$

where  $E_f(N, K)$  is the total number of ways in which none of the  $N$  channels are successful given a total of  $K$  users transmit. Similarly,  $E_s(N, K)$  is the total number of ways in which all the  $N$  channels are successful given a total of  $K$  users transmit. Calculation of  $E_f(N, K)$  and  $E_s(N, K)$  is given in Appendix 5.1.

#### 5.3.1.2 Infinite Users

In the infinite user case the new packet arrival is assumed to be Poisson distributed with mean arrival rate of  $\lambda$ . With the proposed capture model the throughput of an infinite user S-Aloha network is

$$S = \sum_{n=1}^M np(n)p_s(n) \quad (89)$$

where  $p(n)$  is the poisson distribution as given by  $p(n) = e^{-\lambda}\lambda^n/n!$  with mean arrival rate  $\lambda$  and  $p_s(n)$  is the success probability when  $n$  users transmit. For SISO/IC case  $p_s(n) = 1/n$  Using (89), the value of  $\lambda$  for which the network is stable can be obtained.

### 5.3.2 Multi-Packet Reception

#### 5.3.2.1 Frame Structure for Multi-packet Reception

This section proposes the frame structure and capture model for multi-packet reception. A frame consists of preamble and data portions. The base station estimates

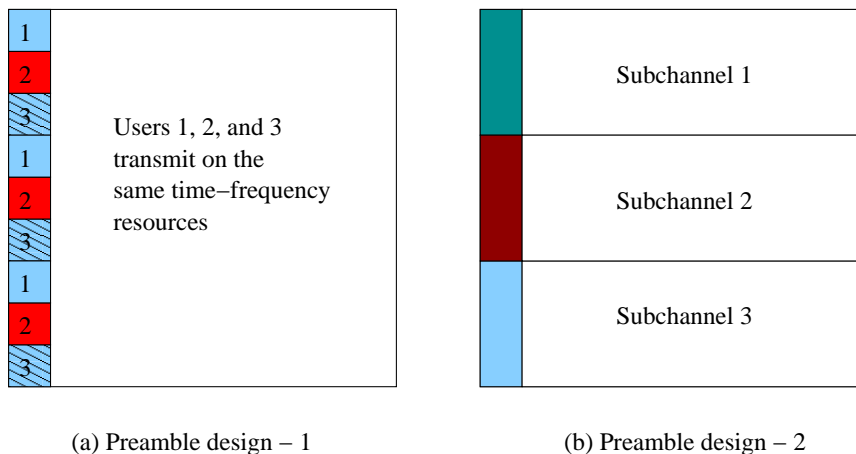


**Figure 15:** Frame structure for MUD

the channel based on the preamble. These channel estimates are then used to compute the beam-forming weight for MPR. To estimate each user’s channel correctly, the effect of interfering users’ signal should be minimized. This is achieved by using orthogonal preambles for each user. Two preamble designs are used to achieve the orthogonality.

- In the first design, the sub-carriers in each band are grouped into clusters consisting of non-overlapping sub-carriers. Figure 15a shows this frame structure. The sub-carriers in any cluster are evenly spaced,  $D (\geq M)$  sub-carriers apart, across the complete band. This enables the users to estimate the channel across the complete band by interpolation. Hence, the system can operate in a frequency selective channel. A user chooses one of the  $D$  clusters, with probability  $1/D$ , to transmit its preamble. All the users can use the same preamble sequence in this design. We assume that all the  $M$  packets will be successfully received if all the users in the same sub-channel occupy different set of sub-carriers in the preamble.
- In the second preamble design, all the users transmit their preamble on all the sub-carriers in their band. Figure 15b shows this frame structure. User orthogonality is attained in this case by choosing orthogonal preamble sequences. There

can be multiple choices for these orthogonal sequences. One design is proposed in the following. Let  $s_k^l$  be the unity norm preamble symbol transmitted on the  $k^{\text{th}}$  sub-carrier by user  $l$ . An orthogonal sequence for user  $m$  is given as

$$s_k^m = s_k^l \exp(j2\pi k\tau_m/N), \quad (90)$$

where,  $N$  is the total number of sub-carriers in the band and  $\tau_m$  is an integer  $\geq 0$  that is different for each user. The orthogonality is simply proved as follows. The cross correlation between the sequences is given as

$$\begin{aligned} (\mathbf{s}^l)^T \mathbf{s}^m &= \sum_{k=0}^{N-1} s_k^l s_k^m \\ &= \sum_{k=0}^{N-1} |s_k^l|^2 \exp(j2\pi k\tau_m/N) = 0 \end{aligned} \quad (91)$$

where  $\mathbf{s}^l = [s_0^l \dots s_{N-1}^l]^T$ . The fact that preamble symbols have unity norm is used to obtain orthogonality. For this design to work well the channel needs to be constant over the  $N$  sub-carriers. To illustrate this, let the received signal, when two users are transmitting, at the  $k^{\text{th}}$  sub-carrier be (interference limited case)

$$y_k = h_1 s_k^1 + h_2 s_k^2 \quad (92)$$

The averaged least squares (LS) channel estimate is

$$\hat{h}_i = \sum_{k=0}^{N-1} y_k s_k^i = h_i \quad (93)$$

It can be easily seen from the above equations that perfect channel estimates can be obtained by averaging if each user  $i$  has preambles with unique  $\tau_i$ . Successful reception of packets using this preamble design requires that (a) No more than  $M$  packets transmit on the same band and (b) when (a) is satisfied only those packets are successfully received whose preamble is orthogonal to all other packet in that band.

In the case of MPR, described above,  $M$  is assumed to be governed by the number of antennas at the base station. Analytical model of success probabilities under finite user scenario for MPR is given next.

### 5.3.2.2 Finite users

The analytical expression of  $P(d|K)$  for preamble design 1 is difficult to compute and has not yet been obtained. Monte carlo simulations are performed to get the results for this design. However,  $P(d|K)$  has been derived for preamble design 2 as given below. Total number of ways for  $d$  successful reception given  $K$  users transmit is given by

$$P(d|K) = \binom{K}{d} \sum_{n_s = \lfloor \frac{d}{M} \rfloor + 1}^{\min(d, NM)} \binom{N}{n_s} \times \frac{E_s(d, n_s) E_f(K - d, N - n_s)}{N^K}, \quad (94)$$

where  $E_f(N, K)$  is defined in the same way as that for SPR and its expression is also the same given by 96 in Appendix 5.6.  $E_s(N, K)$ , however, has a different expression and is derived in Appendix 5.7. It is defined as the number of ways in which  $K$  users are successful and occupy  $n_s$  cells. This derivation includes the SINR-based LMMSE collision model derived in Chapter 3.

### 5.3.3 Performance analysis

The average throughput and delay expressions with capture are exactly the same as those without capture for the case of SPR. In the case of MPR the average throughput expression is slightly modified as follows

$$\bar{D} = \sum_{n=0}^{MN} n Pr\{D_k = n\}. \quad (95)$$

Note that the difference between equations (85) and (95) is in the upper limit of the summation, since with MPR a maximum of  $MN$  packets can be successfully received.

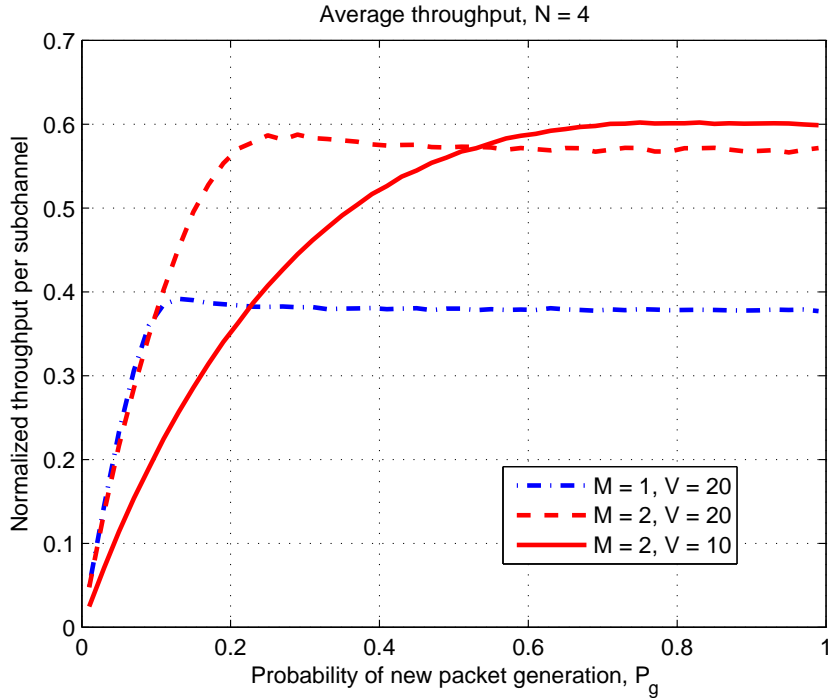


**Figure 16:** Average throughput of multichannel S-ALOHA network with (solid and dashed lines) and without (dash-dotted line) capture for SPR.

## 5.4 Results

This section provides the throughput and delay results of finite user multi-channel S-ALOHA network with capture. Detailed results and discussion are presented for single packet reception scenario and MPR scenario is discussed only briefly. Detailed results and discussion for MPR will be presented in the full paper. Maximum stable throughput (MST) and behavior of average delay can be obtained easily using (89).

Fig. 16 shows the throughput per subchannel with and without capture for single packet reception as a function of  $p_g$ , which is the probability of new packet generation in the network. As is well known, MST of classical S-Aloha is  $1/e$ . This is achieved when 20 users transmit in 4 subchannels. MST when capture is considered increases to  $1.5/e$ , this can be analytically obtained from (89) for infinite user case. One way to look at capture is to assume that the base station has  $M$  antennas and that it can suppress up to  $M - 1$  interferers by using a MUD receiver. Hence, the result can

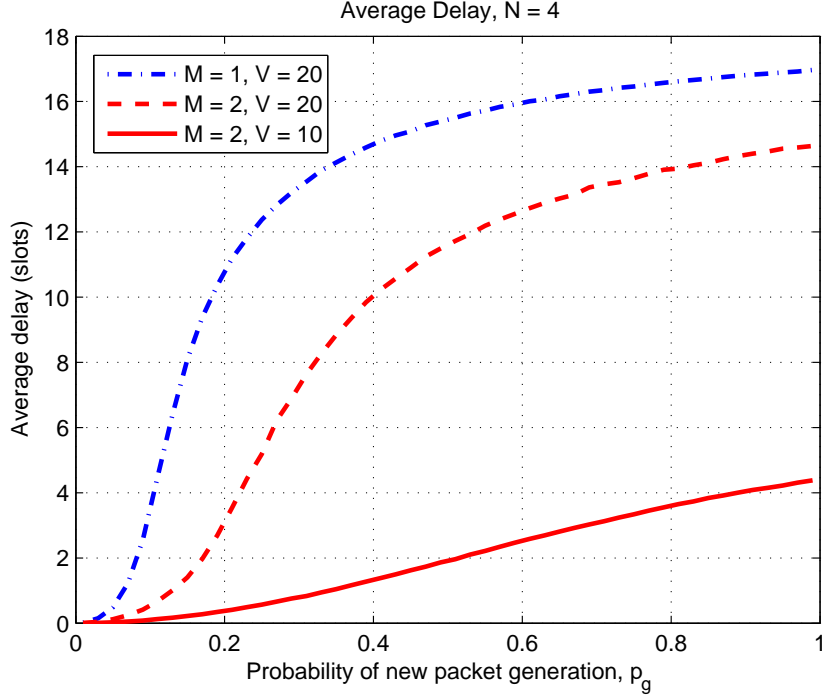


**Figure 17:** Average delay of multichannel S-ALOHA network with (solid and dashed lines) and without (dash-dotted line) capture for SPR.

also be interpreted as the performance gain seen by using multiple antennas. It is noted that when  $p_g < 0.1$  there is no advantage of using a MUD receiver in terms of throughput. It is interesting to note that when there are only 10 users in the network, the MST is slightly higher with capture. Fig. 17 gives average delay for the scenarios discussed above. We note that in the worst case, when operating at MST, the delay is reduced by up to 2 slots. The best delay benefit is obtained when  $p_g = 0.2$ . In this case, the average delay is reduced by about 6 slots because of capture.

Figs. 18 and 19 show stabilized throughput and average delay of a S-Aloha network with MPR using the two preamble designs. The legends Scheme-1 and Scheme-2 correspond to the first and the second preamble designs, respectively. In both the scenarios there are 20 users in the network. The complete band is divided into  $N = 4$  subchannels and up to  $M = 2$  users can be simultaneously received per subchannel. For Scheme-1, the separation between two pilot subcarriers is  $2N$ ; for Scheme-2, the

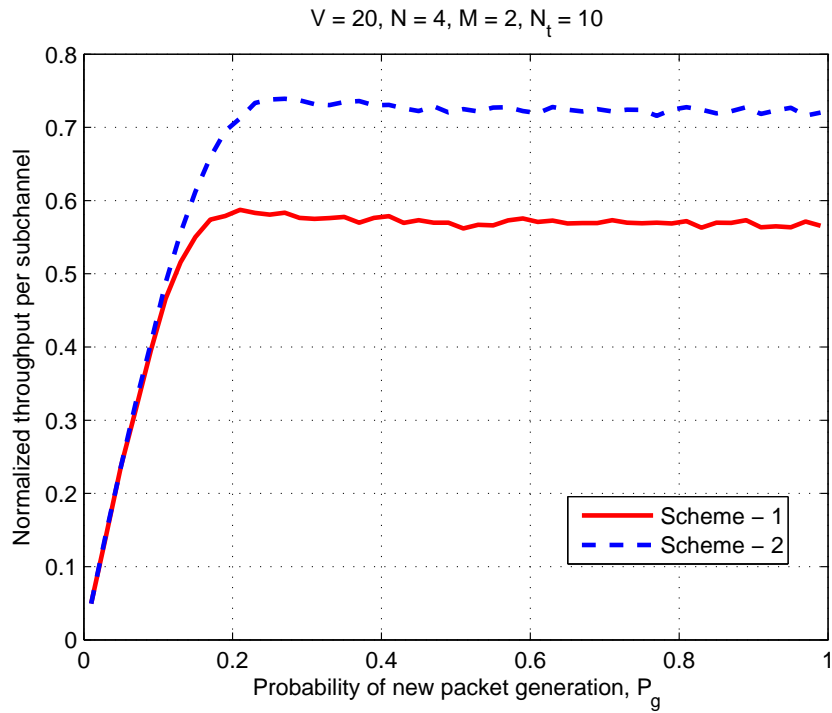


**Figure 18:** Average throughput of multichannel S-Aloha with multiuser detection. Scheme - 1: Decimated preamble, Scheme - 2: Orthogonal training sequences

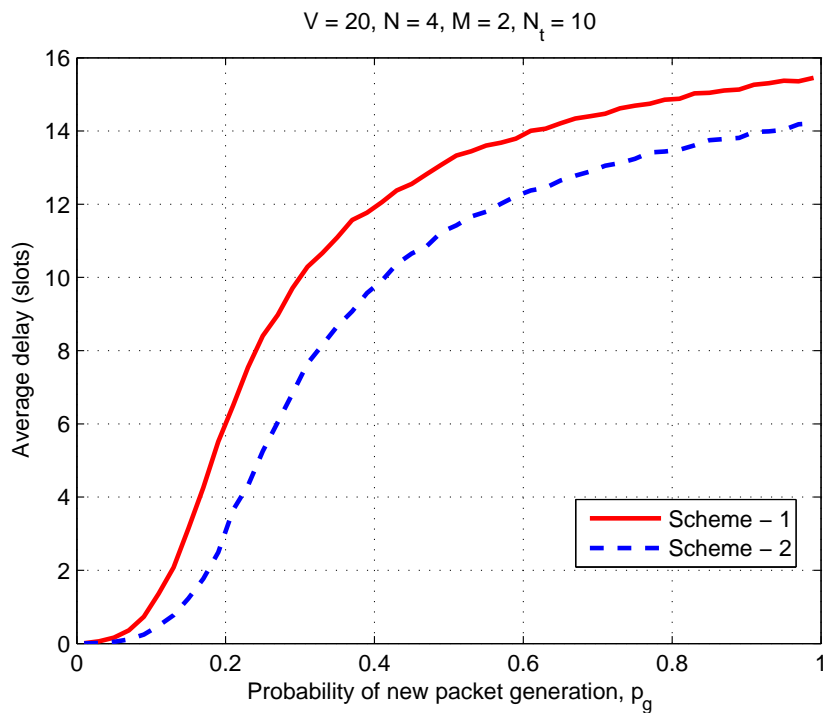


**Figure 19:** Average delay of multichannel S-Aloha with multiuser detection

number of orthogonal preamble sequences,  $N_t = 10$ . Clearly, the Scheme-2 will have a higher success probability because each sub-channel can have different set of 2 user scenarios. Hence, an improved MST compared to Scheme-1. We observe that the MST in Scheme-1 is  $2/e$  where as that for Scheme-2 is  $1.5/e$ . Note that MST remains almost the same with  $p_g \leq 0.1$ . Scheme-1 also has consistently lower average delay by about 1 slot. However, it may be noted that Scheme-2 will not be able to extract any frequency diversity of the channel when coding is used where as Scheme-1 will have this benefit. But this aspect has not been accounted for in the model presented here.

## **5.5 Summary**

In this chapter, a multi-channel stabilized S-Aloha system with capture was modeled. Both single- and multi-packet reception were considered. For single-packet reception case, it was shown that for a lightly loaded system, i.e. when rate of new packet generation in the network is low, there might not be enough advantage to use a multiple antenna system. Also, in a finite user case the MST reduced slightly with increasing number of users this was because the attempts were binomial instead of Poisson. The MST very quickly reached the infinite user case with increasing number of users. The multi-packet reception framework was proposed for multi-antenna base station. Two preamble designs were used to allow multiuser detection. The MST and average delay of networks employing the two types of preambles was compared.

## **5.6 Appendix 5.6**

$E_f(N, K)$  can be easily obtained by observing that each of the  $N$  cells must have at least  $M$  users. Hence, rest of the  $K - NM$  users can be placed arbitrarily in the  $N$

cells and none of the  $N$  cells would have any success. We obtain

$$E_f(N, K) = \sum_{n_f=1}^{\lfloor \frac{K}{M+1} \rfloor} \binom{N}{n_f} \binom{K}{n_f(M+1)} \frac{(n_f(M+1))!}{(M+1)!^{n_f}} n_f^{K-n_f(M+1)} \quad (96)$$

Next, the successful cells can be computed as

$$E_s(N, K) = \binom{K}{N} N!(N^K - E(N, K - N)) \quad (97)$$

where  $E(N, K - N)$  is the total number of ways in which at least one channel has  $M$  or more users. This can be computed using the theorem on union of events as follows

$$E(N, K) = S_1 - S_2 \dots + (-1)^{\nu+1} S_\nu \quad (98)$$

where  $S_\nu$  is the total number of ways in which some  $\nu$  cells have  $> M$  users, it is given as

$$S_\nu = \binom{N}{\nu} \sum_{\mathbf{j}} \binom{K}{\nu M + \mathbf{j}^T \mathbf{1}} \times \frac{\nu M + \mathbf{j}^T \mathbf{1}}{\prod_{k=1}^{\nu} (M + j_k)} (N - \nu)^{K - \nu M - \mathbf{j}^T \mathbf{1}} \quad (99)$$

where  $\nu = \lfloor \frac{K}{M+1} \rfloor$ ,

$$\sum_{\mathbf{j}} = \sum_{j_1=1}^{K_1} \sum_{j_2=1}^{K_2} \sum_{j_\nu=1}^{K_\nu}, \quad \mathbf{j} = [j_1 \ j_2 \ \dots \ j_\nu]^T, \\ \mathbf{1} = \underbrace{[1 \ 1 \ \dots \ 1]^T}_{\nu \text{ times}}$$

and

$$K_1 = K - \nu M - \nu + 1, \\ K_2 = K - \nu M - j_1, \dots, \\ K_\nu = K - \nu M - j_1 \dots - j_\nu$$

The derivation of  $S_\nu$  is as follows. We want to find the total number of events such that at least one cell has greater than  $M$  users. As mentioned earlier we use the property that

$$P(A_1 \cap A_2) = P(A_1) + P(A_2) - P(A_1 \cup A_2). \quad (100)$$

Let  $A_{i_1}^j$  be number of events such that cell  $i_1$  has  $M + j$  users

$$A_{i_1}^j = \binom{K}{M+j} (N-1)^{K-M-j}. \quad (101)$$

Hence, the total number of ways in which cell  $i_1$  has greater than  $M$  users

$$A_{i_1}^j = \sum_{j=1}^{K-M} \binom{K}{M+j} (N-1)^{K-M-j}. \quad (102)$$

The total number of ways in which some 1 cell has greater than  $M$  users is

$$S_1 = \binom{K}{1} \sum_{j=1}^{K-M} \binom{K}{M+j} (N-1)^{K-M-j}. \quad (103)$$

Next, we need to find the number of ways in which at least two cells have greater than  $M$  users. Let  $A_{i_1, i_2}^{j_1, j_2} = A_1^j$  be the total number of events such that cell  $i_1$  contains  $M + j_1$  users and cell  $i_2$  contains  $M + j_2$  users

$$A_1^j = \binom{K}{2M+j_1+j_2} \frac{2M+j_1+j_2}{(M+j_1)!(M+j_2)!} \times (N-2)^{K-2M-j_1-j_2}. \quad (104)$$

Hence, the total number of ways in which some two cells have greater than  $M$  users is

$$S_2 = \binom{N}{2} \sum_{j_1, j_2} \binom{K}{2M+j_1+j_2} \times \frac{2M+j_1+j_2}{(M+j_1)!(M+j_2)!} (N-2)^{K-2M-j_1-j_2}. \quad (105)$$

Similarly, the result for  $\nu$  cells can be obtained as given in (99).

## 5.7 Appendix 5.7

The structure of  $E_s(N, K)$  when using preamble design 2 is similar to that for SPR. The difference being that now the success also depends upon the preamble sequence overlap and LMMSE collision model. The expression is as given below

$$E_s^{MUD}(N, K) = Pr(K \text{ users choose orthogonal preambles}) E_s(N, K), \quad (106)$$

where  $E_s(N, K)$  is given by (97) and

$$Pr(K \text{ users choose orthogonal preambles}) = \frac{1}{\sum_{\alpha} \sum_{j=1}^{n_s} N_t^{\alpha_j}} \left[ \sum_{\alpha} \sum_{j=1}^{n_s} \binom{N_t}{\alpha_j} (Pr(\gamma(\alpha_j) > \gamma_{th}))^{\alpha_j} \right], \quad (107)$$

under the conditions that

$$\begin{aligned} \alpha_j &\leq M, \forall j \quad \text{and} \\ \sum_{j=1}^{n_s} \alpha_j &= K. \end{aligned} \quad (108)$$

$N_t$  is the total number of orthogonal preamble sequences that the users can choose from,  $\alpha_j$  is the number of user in cell  $j$ ,  $\alpha$  is the set of all  $\alpha_j$ 's that satisfy the constraints in (108),  $Pr(\gamma(\alpha_j) > \gamma_{th})$  is the collision model for LMMSE receiver as per (37), and  $\gamma(\alpha_j)$  is the SINR when  $\alpha_j$  users are received simultaneously. The above equation assumes that the users are power controlled such that average received power of all the users is the same.

# CHAPTER VI

## AD HOC NETWORKS

### *6.1 Overview*

Ad hoc networks have been the area of recent interest for a wide range of applications. The set of applications of ad hoc networks ranges from small static networks that are constrained by power sources, to large scale, mobile, highly dynamic networks. Significant examples include establishing dynamic communication for disaster relief efforts, military networks, Mars/Lunar surface exploration, etc. Such network scenarios cannot rely on centralized and organized connectivity. The growth of ad hoc networks is at a very nascent stage. The popular IEEE 802.11 wireless protocol incorporates an ad hoc networking system when no wireless access points are present. This MAC scheme is called DCF. However, this is a very basic ad hoc MAC protocol since it only handles one hop traffic between the source and the destination. Each node transmits and receives data, but does not route anything to and from other nodes in the network.

In addition, the advancement in physical layer design has allowed the use of multiple antennas in wireless radios. Multiple antenna radios along with advanced signal processing techniques offer a continuum of transmitter and receiver design choices. By varying these choices one can achieve a large variety of possibilities that range from improving reliability to increasing the data rate. For fixed reliability and data rate the choice may also enable range extension.

This chapter analyzes the throughput of ad-hoc networks for two types of multiple-input-multiple-output (MIMO) architectures. In the first, both the transmitter and receiver have multiple antenna elements and each transmit antenna element emits an independent data stream; this is the popularly known V-BLAST technique [17]. In

the second, the receivers have multiple antennas, but the transmitters only use one antenna. In this later case, the receiver can receive several users' transmissions at once. This transmission technique has gained interest in cellular networks as well and is referred to as space division multiple access (SDMA) technique. While such a system is harder to design because of the need of coordinating multiple users, it offers the advantage of interference avoidance and throughput improvement by multiuser scheduling. However, interference avoidance and multiuser scheduling are not considered in the thesis. The goal here is to analyze the impact of linear and non-linear receiver processing when using the V-BLAST- or SDMA-based network architecture.

The high degree of flexibility in MIMO architectures makes networks with MIMO physical (PHY) layers excellent candidates for medium access control (MAC)- PHY cross-layer design. The MAC is designed to take the special features of the PHY layer and the states of the channel into account in admission decisions. Cross-layer approaches have been shown to increase the throughputs of networks, compared to conventional approaches [36]-[31]. Most of the research in cross-layer design presents theoretical results with the average analysis for centralized network architectures [36], [11], [38], and [69]. Very little is known about ad-hoc networks especially because the theory becomes intractable for multi-hop networks. To the best of our knowledge there are very few existing works that analyze the performance of a multihop ad-hoc network with anything but a "path-loss only" type PHY layer processing [50]. The authors in [36] have also highlighted the need of a good collision model. Furthermore, there are no works the authors are aware of that provide a good collision model for the MIMO PHY layer. For example, in [31], the collision model is deterministic.

The performance of MIMO depends on the type of receiver signal processing algorithm. We consider two popular receiver processing algorithms, linear minimum

mean squared error (LMMSE) and successive interference cancellation (SIC) (a non-linear technique) [18]. They represent a tradeoff in complexity versus performance [8], with SIC providing better performance because it gives higher diversity gains to the weakest signals. SIC was considered in cross-layer design in [16], however [16] did not consider MIMO.

In this chapter, we analyze the impact of LMMSE and SIC receiver-processing techniques on the throughput of multi-hop ad hoc networks with either single-input multiple-output (SIMO) or MIMO flat fading links. In doing so, we make the following contributions i) collision models for multi-packet reception using MMSE and SIC, and ii) a throughput comparison of two receiver processing techniques on a multi-hop SIMO/MIMO adhoc network with two different MAC protocols.

The first MAC protocol, which we call the simple MAC (S-MAC) protocol, allows a user to transmit from at most one antenna. The receiver is capable of handling  $M$  simultaneous streams, where  $M$  is the number of receiver antennas. The second one is called the collision sense multiple access/collision avoidance allowing  $k$  streams (CSMA/CA( $k$ )) MAC protocol, first proposed in [31]. For this chapter, the protocol requires the same user to transmit all the  $k = M$  streams.

We also consider two power policies [14]. One attempts to force the two protocols to expend equal energy by making the total power within the sensing range constant. This is achieved by maintaining constant power per stream (CPPS). The other power policy constrains each node to transmit the same power, even when only one stream is transmitted. This policy is called constant power per node (CPPN). CPPN results in reduced energy per stream for CSMA/CA( $k$ ), compared to CPPS. For a fair comparison of the two protocols we use range-preserving strategy [68] such that SNR per stream is the same at the boundary of decoding and sensing ranges; this results in CSMA/CA( $k$ ) having smaller ranges due to lower power per stream.

In Section 6.2, we revisit the SINR-based linear and non-linear receiver collision

models developed in Chapter 3 and describe how they are used in the ad hoc network analysis. The two MAC protocols, CSMA/CA( $k$ ) and S-MAC, are also discussed in this section. Ad hoc network configuration and simulation parameters followed by the performance results w.r.t different power schemes, MAC protocols, and receiver designs are given in Section 6.3. Finally, a summary of the Chapter is given in Section 6.4.

## 6.2 Collision models

A SISO collision or multi-packet reception model was proposed [56]. This model discussed the capture probability,  $P_{cap}$ , which is the probability that a packet will be correctly decoded if its signal to interference and noise ratio (SINR) is greater than a preset threshold,  $\gamma_{th}$ :

$$P_{cap} = Pr(SINR \geq \gamma_{th}), \quad (109)$$

$P_{cap}$  depends upon coding and modulation. However, [56] considered only path-loss-dependent received signal strength. Later, a detailed study of capture probability, in presence of multipath, shadowing and the near-far effect was done in [11]. To our best knowledge, almost all the work till now uses the collision model proposed in [81] for PHY layer abstraction to be used with MAC layer [11], [38], and [51]. We will extend this model to LMMSE and SIC receivers.

We consider a MIMO system with  $M$  and  $N$  antennas at the receiver and transmitter respectively and a total of  $L + 1$  transmitters. Fig. 20 shows the receiver under consideration in an ad-hoc wireless network. In Fig. 20  $s_i$  is the BPSK symbol with period  $T_s$ . Though all the links in the figure are MIMO-capable we analyze two special scenarios. In the first, the desired transmitter does VBLAST transmission, i.e. the symbol sequence into the transmitter is converted to  $N$  parallel streams before transmission [18], with  $N = M$  and  $L = 0$ . In the second, each transmitting node excites only a single omnidirectional antenna from the antenna array such that

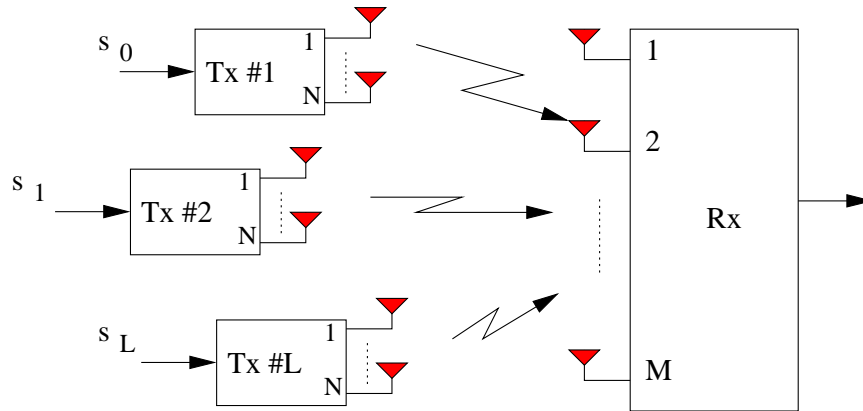


**Figure 20:** Interference scenario in ad-hoc wireless system with V-BLAST transmitters

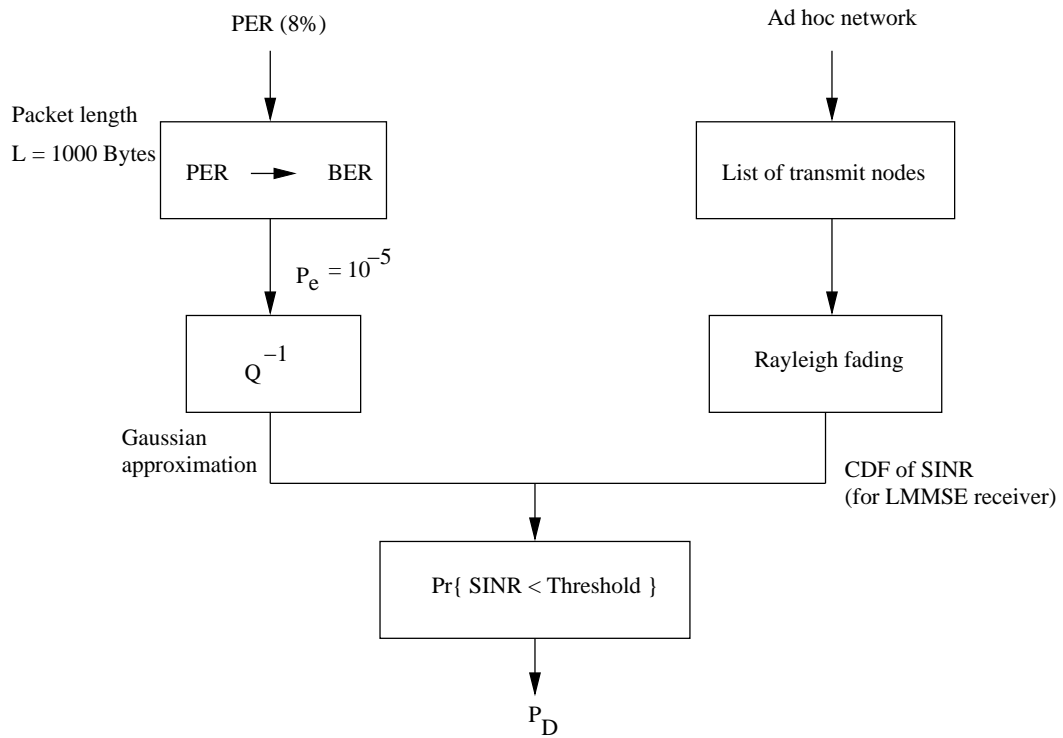


**Figure 21:** Collision model flow chart

$N = 1$  and  $L = M - 1$ ; the antenna is selected deterministically. In both these cases the receiver is fully loaded, which means that the total number of incident streams is equal to the number of receive antennas. For ease of model representation we exploit the fact that even for V-BLAST transmission, all the streams other than the one being demodulated act as interferers. Hence the following system model can be used for both the scenarios

$$\mathbf{x} = \sum_{i=0}^L \alpha_i \mathbf{v}_i s_i + \mathbf{n}, \quad (110)$$

where  $\mathbf{x}$  is a  $M \times 1$  received signal vector,  $\alpha_i$  is the received signal amplitude representing path loss, and  $\mathbf{v}_i$  is a vector of independent unit variance complex rayleigh random variables representing the faded channel of the  $i^{\text{th}}$  stream (first scenario) or  $i^{\text{th}}$  user (second scenario), and  $\mathbf{n}$  is the receiver noise. The desired user is indexed 0.

The post processing SINR of the optimum LMMSE combiner [14] is given by

$$\gamma = \alpha_0 \mathbf{v}_0 \mathbf{\Phi}^{-1} \mathbf{v}_0, \quad (111)$$

where  $\mathbf{\Phi}$  is interference-plus-noise covariance matrix. Assuming noise and interference are uncorrelated and flat fading such that the gain remains constant over the whole packet we have

$$\mathbf{\Phi} = \sigma^2 \mathbf{I} + \sum_{i=1}^L \alpha_i \mathbf{v}_i \mathbf{v}_i^H, \quad (112)$$

where  $\mathbf{I}$  is the identity matrix and we assume that all branches have same noise power.

To compute the probability of packet drop,  $P_D$  we need the cumulative distribution function (CDF) of SINR as a function of fading statistics and path-loss. For this, we apply the approximate semi-analytical solution of the CDF [52] when the total number of incident streams,  $(L + 1) \times N$  is not greater than  $M$ ; such a receiver is called a non-overloaded receiver. Fig. 21 shows the flow chart to compute  $P_D$  at the desired receiver.

The left branch of the flow chart in Fig. 21 shows the relation between the desired PER at the receiver and the threshold for SINR-based collision model. From the

definition of  $P_{cap}$  in 109 we need to define the SINR threshold,  $\gamma_{th}$ , which is determined by the outage probability of the conditional probability of bit error,  $P_e$ . We assume the interference is Gaussian. A simple analysis shows that this assumption provides an upper bound on  $P_e$ . Hence,  $P_D = 1 - P_{cap}$  estimated by this method gives a conservative figure. In this chapter we consider outage to be the case when  $P_e \geq 10^{-5}$  for BPSK modulation. For BPSK modulation,  $P_e$  is given by

$$P_e = Q\left(\sqrt{\frac{2E_b}{N_0}}\right), \quad (113)$$

where  $\gamma = E_b/N_0$  is the SNR per bit.  $\gamma_{th}$  corresponds to a non-faded channel and  $P_e = 10^{-5}$  that we can get by inverting 113:

$$\gamma_{th} = \frac{1}{2} (Q^{-1}(10^{-5}))^2 = 9.12. \quad (114)$$

To compute  $P_D$  we use the post-processor SINR probability distribution function,  $p(\gamma)$  [16], as follows

$$P_D = \int_0^{\gamma_{th}} p(\gamma) d\gamma. \quad (115)$$

A closed form expression for  $P_D$  where different streams have different path losses is difficult to derive. Hence, we generate a table of  $P_D$  for users located on a  $300 \times 300$ m grid with a resolution of 10m, where  $0 \leq k \leq M$ . The reason we choose a maximum of  $M$  streams is because we assume the MAC prevents overloading.

The right hand side of the flow chart in Fig. 21 governs the interference scenario. At the beginning of the  $ns-2$  simulations a network topology is generated by placing the users uniformly in a square block. A centralized scheduler is then used to determine the list of transmitting nodes at a given discrete time of the simulation. The set of active nodes within the sensing range determine the interference pattern. LMMSE and SIC receivers are compared against the ideal receiver that always perfectly decodes all the streams/packets when it is not overloaded. However, when overloaded the ideal receiver rejects all the streams/packets. We note that [9] assumed the ideal receiver model.

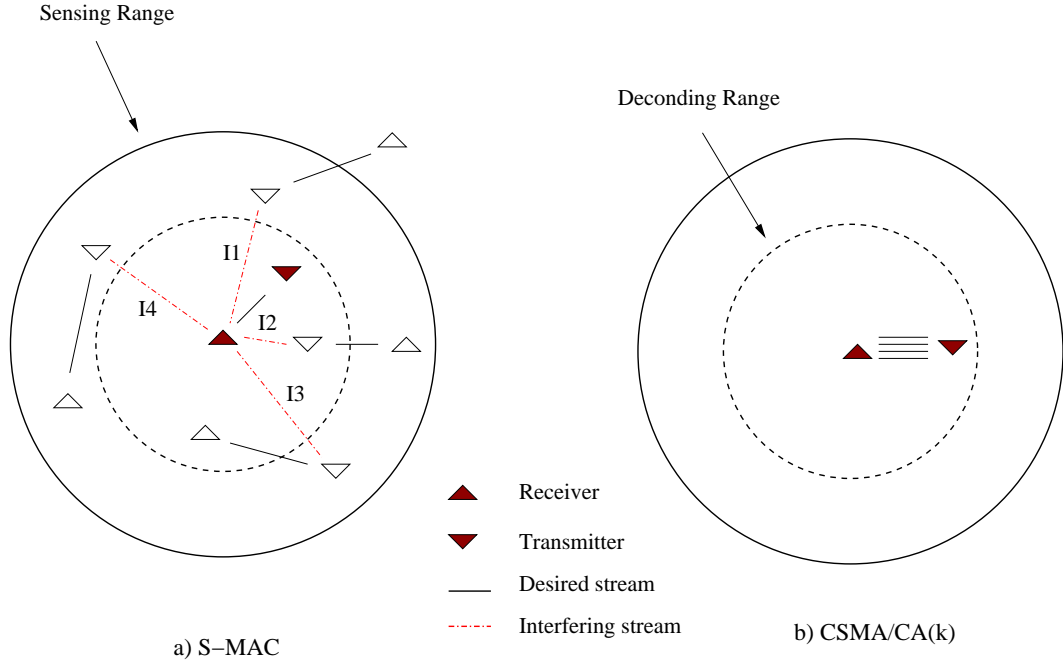


**Figure 22:** Illustration of the two MAC protocols

### 6.2.1 Simple MAC (S-MAC) protocol

S-MAC requires that the desired user is single stream and should be within the decoding range. S-MAC allows a maximum of  $M - 1$  interferers to be anywhere within the sensing range, because the MIMO receiver can suppress them. We assume centralized control in this chapter, so S-MAC never admits more than  $M$  streams within the sensing range of a receiver. However, a distributed version might sometimes erroneously allow receiver overloading. Fig. 22(a) shows the functionality of the distributed S-MAC protocol with  $M = 4$ . The upright triangles represent receivers; the inverted triangles represent transmitters, with filled and unfilled triangles indicating the desired and interfering nodes, respectively. The packet will be dropped with  $P_D = 1$  if all the four interfering links are active, however, if any three of these links are active then the packet will be dropped with the  $P_D$  obtained from the table.

In case of the SIC receiver, the users are sorted based on their average power and canceled in order of descending average power. We assume perfect channel estimation

and cancelation. This implies that the stream demodulated first will not get any diversity gain, the second stream will have a diversity order of 2, third will have order 3 and so on.

### 6.2.2 CSMA/CA( $k$ ) MAC protocol

The CSMA/CA( $k$ ) protocol requires a node to sense the channel before transmitting, and V-BLAST transmission with all  $M$  streams occurs only if the channel is free; otherwise, the transmitter does a back-off and attempts VBLAST transmission after a random back-off time [2]. Fig. 22(b) shows the functionality of CSMA/CA( $k$ ). This protocol is conservative in the sense that it does not allow any transmissions in the sensing range; only the desired user within the decoding range is allowed to transmit. All  $M$  streams must be demodulated without error for the packet to be correctly received. Also it needs to be noted that average power of all the  $M$  streams will be same since they are coming from the same transmitter. When the MMSE receiver is analyzed, the capture probability  $P_{cap}^{MMSE-k} = P_{cap}^M$ , where  $P_{cap}$  is capture probability of one stream, and it is obtained from the table described earlier. Here we have assumed that all the streams are independent of each other (V-BLAST). In case of a SIC receiver, the capture probability,  $P_{cap}^{SIC-k}$ , is given by

$$P_{cap}^{SIC-k} = \prod_{i=1}^M P_{cap}^i, \quad (116)$$

where  $P_{cap}^i$  is the capture probability of the  $i^{th}$  stream given that other  $i - 1$  streams are demodulated.

Performance of the receivers in the network is analyzed using flow throughput. Here a flow is defined as the collection of all the links between desired transmitter and receiver. The flow throughput is defined as the throughput of the bottleneck link. We assume that each stream is transmitted at a rate of 1 Mbps, and a packet is 8ms long. Therefore, under S-MAC each packet contains 1000 Bytes, and under CSMA/CA( $k$ ), each packet contains  $M \times 1000$  Bytes  $M = 4$  is used for the results in

this chapter. We analyze network throughput as a function of network load. Network load is defined as number of active transmitter-receiver pairs.

### ***6.3 Simulation and results***

The received signal power is computed according to a two-slope partitioned model [15] where links with distances less than  $d_b$  have a free space path loss exponent,  $n_1 = 2$ .  $d_b$  is the longest distance between the transmitter and receiver for which first Fresnel Zone does not touch the flat ground. For additional distance beyond  $d_b$ , the path loss exponent is  $n_2 = 3.5$ . For these simulations, we assume that the transmitter and receiver heights are 1.5 m and the center frequency is 2.4 GHz; therefore,  $d_b = 200\text{m}$ .

In our CPPS simulations, the transmit power is 0.4mW per stream, hence the total power in the sensing range is 1.6mW for both the protocols. Under CPPN, each node transmits 0.4mW; therefore under S-MAC, each stream is transmitted with 0.4mW and under CSMA/CA( $k$ ), each stream is transmitted with 0.1mW. The noise spectral density is assumed to be -103.98dBm.

Under CPPN, the nodes have a decoding range of 101m and a sensing range of 202m for CSMA/CA( $k$ ). This corresponds to  $P_D = 0.04$  at 101m and  $P_D = 0.14$  at 202m. The other combinations of the MAC protocol and power schemes have the decoding and sensing ranges equal to 200m and 300m respectively. There are 100 nodes in the network.  $P_D$  is chosen based on the distance of the transmitters from the receiver in the decoding range and is mapped to the closest distance in the grid.

Fig. 23 shows throughput versus load for the CPPS power scheme. We observe that both the MAC protocols have almost the same performance as for the ideal receiver. Also, SIC performs significantly better than LMMSE (around 35%). S-MAC and CSMA/CA( $k$ ) perform similarly because the total data transmission power within the sensing range for the two protocols is the same. SIC performs about as well

as the ideal receiver because we have set the decoding ranges for SIC and LMMSE to be the same, even though SIC performs much better than LMMSE, especially with perfect channel estimation and cancellation. This means that most SIC links will have  $P_e \ll 10^{-5}$ .

Fig. 24 shows throughput versus load for the CPPN power scheme. We observe that CSMA/CA( $k$ ) performs better than the S-MAC for both SIC and LMMSE. As in the CPPS case, SIC performs as well as ideal receiver. Also, SIC throughput is better than LMMSE by about 35% for CSMA/CA( $k$ ) and by about 47% for S-MAC.

We observe that S-MAC under the two power schemes give the same throughput because the notion of stream and node is same for this protocol.

It is interesting to observe that SIC with CSMA/CA( $k$ ) performs so much better than SIC with S-MAC (by about 100%). This seems to contradict the physical layer knowledge that SIC benefits from the stream power disparity [17] that naturally results from S-MAC. We had also observed that a stream control strategy similar to S-MAC outperformed CSMA/CA( $k$ ) for a toy network, using a throughput definition based on Shannon capacity [18]. We attribute the contrary results in this chapter to the higher spatial reuse in a large multi-hop network that results from the smaller decoding and sensing ranges of CSMA/CA( $k$ ) under CPPN, because shortening range is known to increase throughput in ad hoc networks [21].

We anticipate that under CPPS we might see more of a gap between SIC-S-MAC and SIC-CSMA/CA( $k$ ) if we shorten the decoding range, so that  $P_D$  has more of an impact on throughput. Another important consideration not investigated in this chapter that may give SIC-S-MAC a stronger advantage over SIC-CSMA/CA( $k$ ) is that SMAC can be combined with selection diversity at the transmitter for a small cost in signaling overhead [19], or with space-time block coding transmit diversity [20] for an additional complexity cost in the receiver signal processing.

The CPPN results in Fig. 24 show an interesting cost performance trade-off,

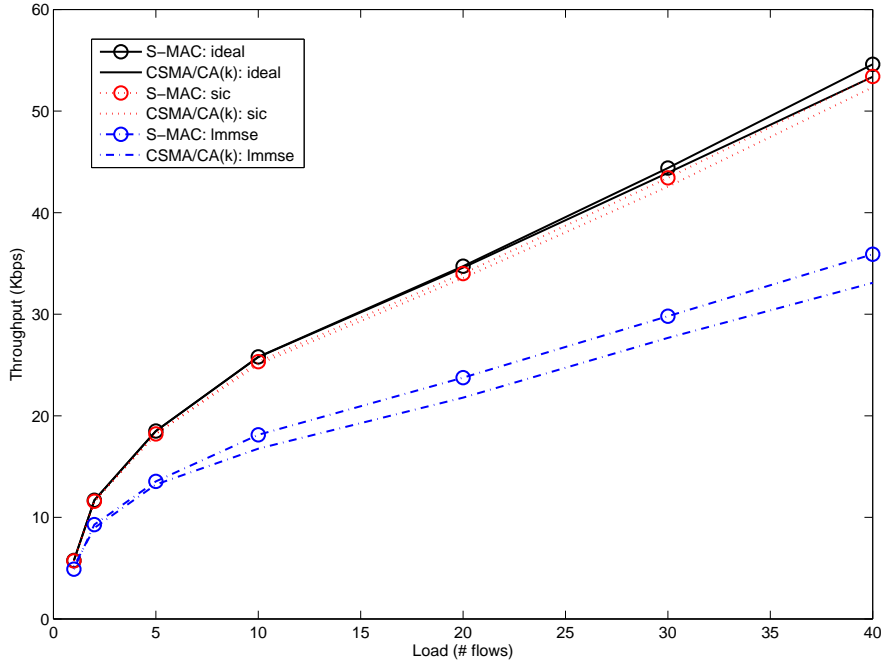


**Figure 23:** Throughput of an ad-hoc wireless network employing ideal, SIC, and LMMSE receivers with CPPS power scheme

in that the less complex (and hence less expensive) Linear MMSE receiver with CSMA/CA( $k$ ) can perform better than the more complex non-linear SIC with S-MAC when employed in a large multi-hop ad hoc network.

S-MAC can be generalized to allow more than one stream per user [2,18]. The advantage of using such a scheme is that some links in the network can allocate more resources if they need a higher data rate. The disadvantage is that a small overhead is required to inform the transmitter how many streams it can transmit. We anticipate that the throughput in this case would lie in between the S-MAC (single stream case) and CSMA/CA( $k$ ) (all streams case).

## 6.4 Summary

We proposed a collision model for the study of a multi-hop MIMO ad-hoc wireless network. Network throughputs were compared for LMMSE, SIC, and ideal receivers,

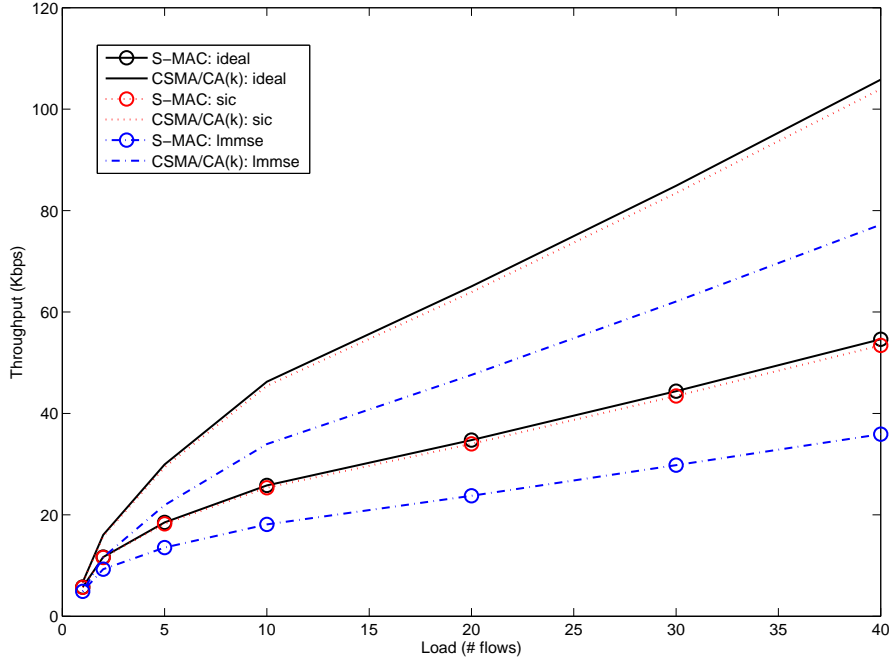


**Figure 24:** Throughput of an ad-hoc wireless network employing ideal, SIC, and LMMSE receivers with CPPN power scheme

for CSMA/CA( $k$ ) and S-MAC protocols, and for CPPS and CPPN power schemes. We concluded that SIC and CSMA/CA( $k$ ) is a high-throughput combination under a CPPN constraint, because of the spatial reuse in large multi-hop networks. We showed that power scheme had significant impact on the network performance. With CPPS, the two MAC protocols had very similar behavior but the receiver processing had an impact. With CPPN, both MAC protocol and receiver processing played important roles.

Although SIC and CSMA/CA( $k$ ) was a powerful combination it would have a higher number of hops on average to reach the destination because of shorter decoding range, which could negatively impact time sensitive applications such as video streaming. Also, this work considers a flat fading channel, and therefore does not capture the diversity advantage of wideband channels under frequency selective fading. It would be useful to address these issues in future.

# CHAPTER VII

## SUMMARY AND FUTURE RESEARCH

In this chapter, we summarize the research results and contributions, and suggest directions for the future work.

### *7.1 Research Summary*

In this thesis, collision models for LMMSE-based linear and non-linear receivers have been developed. These collision models were then used in modeling the effect of physical layer processing in a random access cellular network and an ad hoc network. The results thus obtained helped us develop a deeper understanding of the interaction of PHY and MAC layers. The following are the main contributions of this research:

1. **Physical layer abstraction** [60], [62]: A simple closed form expression of the SINR CDF and ABER of an LMMSE receiver was derived. This work first derived an approximate closed form expression (CFE) of the average eigenvalues of a random interference covariance matrix when the interferers are Rayleigh faded. The approximate CFEs derived in this paper were then used to obtain simple CFEs for the CDF of the SINR and the ABER of an LMMSE receiver in a flat Rayleigh fading channel. Transmissions from one desired and two interfering users were considered. All the three users were allowed to have different average powers at the receiver. The result, with slight modification, could also be applied to a two antenna LMMSE receiver with any number of equal average power users. The benefit of these expressions is that they can be used in analytical models of the networks employing LMMSE receivers to obtain deeper understanding of the impact of physical layer processing on the network performance. The semi-analytical expression developed in [52] may be used for scenarios that are not covered by the simple CFEs.

Further, an SINR-based collision model of an LMMSE-DF MUD was developed. This model assumed perfect cancelation. It could be applied to a receiver in a network with SM or SDMA transmissions.

The last contribution on this topic was an ABER-based collision model of an LMMSE receiver. Effect of packet length, modulation, and coding can be captured by this model. However, it is accurate only at low BERs since it uses only the first order terms in the Taylor series expansion of packet error rate which is a function of BER.

**2. Linear spatial processing in an S-ALOHA-based random access network** [58], [59], [63]: This work consists of two parts:

- i. The SINR- and ABER-based collision models of LMMSE receiver developed in this thesis were used to derive an analytical model for the analysis of an S-Aloha network employing a multiple antenna LMMSE receiver [59]. A closed form expression of the throughput of S-ALOHA network using a two antenna LMMSE receiver was derived. Throughput of such a network was analyzed under a Rayleigh channel condition without power disparity.
- ii. An analytical model was derived for a multi-channel stabilized S-Aloha system with capture [58], [63]. A capture model for single packet reception in a multi-carrier stabilized S-Aloha network was first developed. This model can be effectively used for both single and multiple antenna base station. A multi-packet reception model was also developed for a multi-antenna base station. In this model, the base station can use a minimum mean square error (MMSE) receiver. Two frame structures have been used to allow multiuser detection by MMSE processing. The two frame structures use popular designs of preamble to ensure orthogonality between the users for respective channel estimation. It

was shown that for a lightly loaded system, i.e. when rate of new packet generation in the network is low, there might not be enough advantage to use a multiple antenna system in terms of throughput. It was also shown that in a finite user case the maximum attainable stabilized throughput reduces slightly with increasing number of users and very quickly reaches the infinite user case. The higher throughput with fewer users in the network is because the transmission attempts are binomial instead of Poisson, which is the case with infinite number of users.

### 3. **Linear and non-linear spatial processing in multi-hop ad hoc network**

[21]: Effect of LMMSE and SIC receivers in a multi-hop ad hoc network, was investigated. A novel MAC for ad hoc networks called S-MAC was proposed. This MAC essentially allows SDMA transmissions. Its performance was compared against CSMA/CA( $k$ ), which is the extension of standard CSMA/CA MAC for MIMO SM [31]. The SINR-based collision models for LMMSE and LMMSE-DF receivers developed in this thesis was used for the study of a multi-hop MIMO ad-hoc wireless network. Network throughput was compared for LMMSE, SIC, and ideal receivers, for CSMA/CA( $k$ ) and S-MAC protocols, and for CPPS and CPPN power schemes. It was concluded that SIC and CSMA/CA( $k$ ) is a high-throughput combination under a CPPN constraint, because of the spatial reuse in large multi-hop networks. We show that power scheme has significant impact on the network performance.

## **7.2 *Future work***

All the work in this thesis considers an un-coded system. However, almost all the existing wireless systems are coded. It will be very useful to develop models that capture the effect of forward error correcting codes. It is hard to develop exact analytical models for the error correcting codes. Two techniques may be followed to

approximately capture the effect of coding.

One of the popular techniques called EESM is discussed in Chapter I. This technique fits in very well as an extension of the work in this thesis, since the input to EESM is the post spatial processing SINR at the receiver, which is the SINR that has been used in the collision models in the thesis. The EESM is a channel-dependent function that maps power level and modulation and coding scheme level to SINR values in the AWGN channel domain. This allows using this mapping along with AWGN assumptions. This technique capture the effect of actual codes, eg. Turbo code, convolutional code, etc, along with the modulation in a frequency selective channel.

Another method that can be used is based on channel capacity formulation and use of sphere packing bounds [43] and [44]. Unlike the EESM approach, using the sphere packing bound does not model a real coding and modulation scheme. It just provides a lower bound on the performance of a coded system.

Once the capture models for the coded system are developed they can be applied not only to the random access cellular and the ad hoc networks but also to other networks of interest like the mesh and the conventional cellular networks.

## REFERENCES

- [1] *The ns manual*. The VINT Project.
- [2] *IEEE Standard for Local and Metropolitan Area Networks, Amendment 2: Physical and Medium Access Control Layers for Combined Fixed and Mobile Operation in Licensed Bands*. IEEE Std 802.16e-2005.
- [3] *IEEE Standards for Information Technology, Telecommunications and Information Exchange between Systems, Local and Metropolitan Area Network - Specific Requirements, Part 11: Wireless LAN Medium Access Control (MAC) and Physical Layer (PHY) Specifications*. IEEE Std 802.11.
- [4] *P802.11N (D2) Draft STANDARD for Information Technology, Part 11: Wireless LAN Medium Access Control (MAC) and Physical Layer (PHY) specifications: Amendment : Enhancements for Higher Throughput*. IEEE Std 802.11.
- [5] *TS 25.214 3rd Generation Partnership Project, Physical layer procedures (FDD). V3.2.1. 3GPP PHY*.
- [6] A. R. S. BAHAI, B. R. S. and ERGEN, M., *Multicarrier digital communications: theory and applications of OFDM*. Springer Media Inc., 2004.
- [7] ABRAMSON, N., “The throughput of packet broadcasting channels,” *IEEE Trans. on Communications*, vol. 25, pp. 117–128, Jan. 1977.
- [8] AL-SEMARI, S. A. and GRAMI, N., “A general expression for the capacity of slotted aloha under nakagami fading,” in *IEEE Wireless Communications and Networking Conference*, vol. 2, pp. 849–853, Sept. 1999.
- [9] ARNBAK, J. C. and BLITTERSWIJK, W. V., “Capacity of slotted aloha in rayleigh-fading channels,” *IEEE Journal on Selected Areas in Communications*, vol. 53, pp. 261–269, Feb. 1987.
- [10] B. CLASSON, P. SARTORI, Y. B. K. B. R. L. Y. S., “Efficient ofdm-harq system evaluation using a recursive eesm link error prediction,” in *IEEE Wireless Communications and Networking Conference*, vol. 4, pp. 1860–1865, Apr. 2006.
- [11] B. HAJEK, A. K. and LAMAIRE, R. O., “On the capture probability for a large number of stations,” vol. 45, pp. 254–260, Feb. 1997.
- [12] BERTSEKAS, D. and GALLAGER, R., *Data Networks*. Prentice Hall, 1987.
- [13] D. DARDARI, V. T. and VERDONE, R., “On the capacity of slotted aloha with rayleigh fading: the role played by the number of interferers,” *IEEE Communication Letters*, vol. 4, pp. 155–157, May. 2000.

- [14] DEMIRKOL, M. and INGRAM, M., “Stream control in networks with interfering mimo links,” in *IEEE Wireless Communications and Networking Conference*, vol. 1, pp. 343–348, Mar. 2003.
- [15] DURGIN, G. D., *Space-time wireless channels*. Prentice-Hall, 2003.
- [16] E. D. LENTZ, J. Z., “Joint scheduling and interference cancellation in ad-hoc networks,” in *IEEE Military Communications Conference*, vol. 1, pp. 711–715, Oct. 2003.
- [17] FOSCHINI, J. G., “Layered space-time architecture for wireless communication in a fading environment when using multi element antennas,” *Bell Labs Technical Journal*, 1996.
- [18] G.D. GOLDEN, C.J. FOSCHINI, R. V. and WOLNIANSKY, P., “Detection algorithm and initial laboratory results using v-blast space-time communication architecture,” vol. 35, pp. 14–16, Jan. 1999.
- [19] GERLA, M. and KLEINROCK, L., “Closed loop stability controls for s-aloha satellite communications,” *Proceedings of the Fifth Data COmmunications Symposium*, pp. 2.10–2.19, Sep. 1977.
- [20] GITMAN, I., “On the capacity of slotted aloha networks and some design problems,” *IEEE Trans. on Communications*, vol. 23, pp. 305–317, Mar. 1975.
- [21] H. SHEKHAR, K. SUNDARESAN, M. A. I. and SIVAKUMAR, R., “Linear and non-linear receiver processing in mimo ad hoc network,” in *8th International Symposium Wireless Personal Multimedia Communications*, Dec. 2005.
- [22] H. SHEKHAR, K. SUNDARESAN, M. A. I. and SIVAKUMAR, R., “Linear and non-linear receiver processing in mimo ad hoc networks,” in *Wireless Personal and Mobile Communication*, vol. 1, Nov. 2005.
- [23] HAJEK, B. and LOON, T. V., “Decentralized dynamic control of a multiaccess broadcast channel,” *IEEE Trans. Automat. Contr.*, vol. AC-27, pp. 559–569, Jun. 1982.
- [24] I. KOO, S. S. and KIM, K., “Performance analysis of random access channel in ofdma systems,” in *Proceedings of the 2005 Systems Communication*, pp. ?–?, Mar. 2005.
- [25] J. ANDREWS, A. G. and MUHAMED, R., *Fundamentals of WiMAX: understanding broadband wireless networking*. Prentice-Hall, 2007.
- [26] J. R. BARRY, E. A. L. and MESSERSCHMITT, D. G., *Digital communication*. Kluwer Academic Publishers, 2003.
- [27] J. WARD, R. T. C., “Improving the performance of a slotted aloha packet radio network with an adaptive array,” *IEEE Trans. on Communications*, vol. 40, pp. 292–300, Feb. 1992.

- [28] J. WARD, R. T. C., “High throughput s-aloha packet radio networks with adaptive antennas,” *IEEE Trans. on Communications*, vol. 41, pp. 460–470, Mar. 1993.
- [29] JIAN LI, P. S. and WANG, Z., “On robust capon beamforming and diagonal loading,” *IEEE Trans. on Signal Processing*, vol. 51, pp. 1702–1715, Jul. 2003.
- [30] K. BRUVOLD, E. A., “A qos framework for stabilized collision channels with multiuser detection,” in *IEEE International Conf. on Communications*, vol. 1, pp. 250–254, May 2005.
- [31] K. SUNDARESAN, R. SIVAKUMAR, M. A. I. and CHANG, T.-Y., “A fair medium access control protocol for ad-hoc networks with mimo links,” in *23<sup>rd</sup> Annual Joint Conference of the IEEE Computer and Communications Societies*, vol. 4, pp. 2559–2570, Mar. 2004.
- [32] K. ZHANG, K. PAHLAVAN, R. G., “Slotted aloha radio networks with psk modulation in rayleigh fading channels,” *Electronics Letters*, vol. 25, pp. 412–413, Mar. 1989.
- [33] KANG, H., *Multiple antenna systems in a mobile-to-mobile environment*. Ph.D. Dissertation, 2006.
- [34] KANG, M., “Performance analysis of mimo systems in presence of co-channel interference and additive gaussian noise,” in *Proc. 37<sup>th</sup> Annual Conference on Information Sciences and Systems*, pp. ?–?, Mar. 2003.
- [35] L. D. TOSHNIWAL, R. RADHAKRISHNAN, R. A. and CAFFERY, J., “A novel mac layer protocol for space division multiple access in wireless ad hoc networks,” in *Eleventh International Conf. on Computer Communications and Networks*, vol. 1, pp. 614–619, Oct. 2002.
- [36] L. TONG, V. N. and VENKITASUBRAMANIAM, P., “Signal processing in random access,” vol. 21, pp. 29–39, Sept. 2004.
- [37] L. WANG, S. H. and CHEN, A., “Interference cancellation for downlink tdma systems using smart antennas,” in *IEEE Wireless Communication and Networking Conference*, vol. 4, pp. 2233–2237, Dec. 1999.
- [38] L. WANG, S. H. and CHEN, A., “On the throughput performance of csma-based wireless local area network with directional antennas and capture effect: A cross-layer analytical approach,” in *IEEE Wireless Communication and Networking Conference*, vol. 3, pp. 1879–1884, Mar. 2004.
- [39] LARSSON, E. and STOICA, P., *Space-Time Block Coding for Wireless Communications*. Cambridge University Press, 2003.

- [40] M. CHIANI, M. Z. WIN, A. Z. and WINTERS, J. H., "A laguerre polynomial-based bound on the symbol error probability for adaptive antennas with optimum combining," *IEEE Trans. on Wireless Communications*, vol. 3, pp. ?-?, Jan. 2004.
- [41] M. CHIANI, M. Z. WIN, A. Z. R. K. M. and WINTERS, J., "Bounds and approximations for optimum combining of signals in the presence of multiple co-channel interferers and thermal noise," *IEEE Trans. on Communications*, vol. 51, pp. ?-?, Feb. 2003.
- [42] M. CHIANI, M. Z. W. and ZANELLA, A., "The distribution of eigenvalues for correlated wishart matrices applied to optimum combining with unequal power interferers and noise," *IEEE Procs. Information Theory Workshop*, pp. 203–205, Apr. 2003.
- [43] M. FOZUNBAL, S. W. M. and SCHAFER, R. W., "A sphere packing bound on rayleigh block-fading mimo channels," *IEEE International Conf. on Communications*, vol. 5, pp. 3011–3015, May 2003.
- [44] M. FOZUNBAL, S. W. M. and SCHAFER, R. W., "On space time frequency coding over mimo ofdm systems," *IEEE Trans. on Wireless Communications*, vol. 4, pp. 320–331, Jan. 2005.
- [45] M. K. TSATSANIS, R. Z. and BANERJEE, S., "Network-assisted for random access wireless networks," *IEEE Trans. on Signal Processing*, vol. 48, pp. 702–711, Mar. 2000.
- [46] MALLIK, R. K., "The pseudo-wishart distribution and its application to mimo systems," *IEEE Trans. on Information Theory*, vol. 49, pp. ?-?, Oct. 2003.
- [47] MONZINGO, R. A. and MILLER, T. W., *Introduction to adaptive arrays*. Scitech, 2000.
- [48] NAMISLO, C., "Analysis of mobile radio slotted aloha network," *IEEE Journal on Selected Areas in Communications*, vol. 2, pp. 583–588, Jul. 1984.
- [49] NEE, R. V. and PRASAD, R., *OFDM for wireless multimedia communications*. Artech House Publishers, 2000.
- [50] P. P. PHAM, S. P. and JAYASURIYA, A., "New cross-layer design approach to ad hoc networks under rayleigh fading," vol. 23, pp. 28–39, Jan. 2005.
- [51] P. VENKITASUBRAMANIAM, S. A. and L.TONG, "Sensor networks with mobile access: optimal random access and coding," vol. 22, pp. 1058–1068, Aug. 2004.
- [52] PHAM, T. D. and BALMAIN, K. G., "Multipath performance of adaptive antennas with multiple interferers and correlated fadings," *IEEE Trans. on Vehicular Technology*, vol. 8, pp. ?-?, March 1999.

- [53] P.W. WOLNIANSKY, G. J. FOSCHINI, G. G. R. A. V., “V-blast: an architecture for realizing very high data rates over the rich-scattering wireless channel,” *International Symposium on Signals, Systems, and Electronics*, pp. 295–300, Oct. 1998.
- [54] R. PRASAD, R. D. J. VAN NEE, R. N. V. W., “Performance analysis of multiple access techniques for land-mobile satellite communications,” in *IEEE Global Telecommunications Conf.*, vol. 2, pp. 740–744, Dec. 1994.
- [55] RIVEST, R. L., “Network control by bayesian broadcast,” *IEEE Trans. on Information Theory*, vol. IT-33, pp. 323–328, May 1987.
- [56] S. GHEZ, S. V. and SCHWARTZ, S. C., “Stability properties of slotted aloha with multipacket reception capability,” vol. 33, pp. 640–649, Jul. 1988.
- [57] S. KIM, E. A., “Uplink capacity maximization based on random access channel (rach) parameters in wcdma,” in *IEEE Vehicular Technology Conference*, vol. 2, pp. 548–552, May. 2006.
- [58] SHEKHAR, H. and INGRAM, M. A., “Closed form throughput of a s-aloha network using lmmse receiver,” in *41<sup>st</sup> Annual Asilomar Conference on Signals, Systems, and Computers*, Nov. 2007.
- [59] SHEKHAR, H. and INGRAM, M. A., “Closed form throughput of a slotted aloha network using lmmse receiver,” in *to be published in IEEE Asilomar Conf. on Signals, Systems, and Computers*, Nov. 2007.
- [60] SHEKHAR, H. and INGRAM, M. A., “A simple model of lmmse array receiver for network simulation,” *Submitted to IEEE Trans. Wireless Commun*, 2007.
- [61] SHEKHAR, H. and INGRAM, M. A., “Single and multiple packet reception in a random access ofdma system,” in *to be published in 10th International Symposium Wireless Personal Multimedia Communications*, Dec. 2007.
- [62] SHEKHAR, H. and INGRAM, M. A., “Approximate average eigenvalues of a random matrix and their application to lmmse receiver analysis,” in *Submitted to IEEE Radio and Wireless Symposium 2008*, Jan. 2008.
- [63] SHEKHAR, H. and INGRAM, M. A., “On the use of lmmse receiver for single and multiple packet reception in stabilized multi-channel slotted aloha,” in *Submitted to IEEE Radio and Wireless Symposium 2008*, Jan. 2008.
- [64] SHEN, D. and LI, V. O. K., “Stabilized multi-channel aloha for wireless ofdm networks,” in *IEEE Global Telecommunications Conf.*, vol. 1, pp. 701–705, Nov. 2002.
- [65] SHEN, D. and LI, V. O. K., “Performance analysis of a stabilized multi-channel slotted aloha algorithm,” in *IEEE Intl. Symp. on Personal, Indoor, and Mobile Radio Communications*, vol. 1, pp. 249–253, Sept. 2003.

- [66] STRANG, G., *Linear algebra and its applications*. Wellesley-Cambridge press, 2006.
- [67] STUBER, G. L., *Principles of mobile communication*. Kluwer Academic Publishers, 2000.
- [68] SUNDARESAN, K. and SIVAKUMAR, R., “A unified mac layer framework for ad-hoc networks with smart antennas,” in *ACM International Symposium on Mobile Ad hoc Networking and Computing (MOBIHOC)*, May. 2004.
- [69] TONG, L. and NAWARE, V., “Using queue statistics in beamforming for aloha,” in *The Asilomar conference on signals, systems and computers*, vol. 1, pp. 212–215, Nov. 2003.
- [70] TREES, H. L. V., *Detection, estimation and modulation theory, part IV, optimum array processing*. Wiley-Interscience, 2002.
- [71] TSE, D. and VISWANATH, P., *Fundamentals of wireless communication*. Cambridge University Press, 2005.
- [72] TULINO, A. M. and VERDU, S., *Random matrices and wireless communication*. Foundations and Trends in Communications and Information Theory, 2004.
- [73] VUKOVIC, I. N. and BROWN, T., “Performance analysis of the random access channel (rach) in wcdma,” in *IEEE Vehicular Technology Conference*, vol. 1, pp. 532–536, May. 2001.
- [74] WESTMAN, E., *Calibration and evaluation of the exponential effective SINR mapping (EESM) in 802.16*. Master’s degree project, 2006.
- [75] WIN, M. Z. and WINTERS, J. H., “Analysis of hybrid selection/maximal-ratio combining in rayleigh fading,” in *IEEE International Conf. on Communications*, vol. 1, pp. 6–10, Jun. 199.
- [76] WINTERS, J. H., “Optimum combining in digital mobile radio with cochannel interference,” vol. 33, pp. 144–155, Aug. 1984.
- [77] Y. J. CHOI, S. P. and BHAK, S., “Multichannel random access in ofdma wireless networks,” *IEEE Journal on Selected Areas in Communications*, vol. 24, pp. 603–613, Mar. 2006.
- [78] YANG, H. and ALOUINI, M. S., “Throughput of slotted aloha systems in mixed rician-nakagami fading environments with a minimum signal power constraint,” *IEEE International Conf. on Communications*, vol. 6, pp. 1723–1727, Jun. 2001.
- [79] YUE, W., “The effect of capture on the performance of multichannel s-aloha systems,” *IEEE Trans. on Signal Processing*, vol. 39, pp. 818–822, Jun. 1991.

- [80] ZHANG, K. and PAHLAVAN, K., “Relation between transmission and throughput of slotted aloha local packet radio networks,” *IEEE Trans. on Communications*, vol. 40, pp. 577–583, Mar. 1992.
- [81] ZORZI, M. and RAO, R. R., “Capture and retransmission control in mobile radio,” vol. 12, pp. 1289–1298, Oct. 1994.

## VITA

Hemabh Shekhar was born in Bhagalpur, India, on May 27, 1978. He received Bachelor of Technology (Instrumentation) degree from Indian Institute of Technology, Kharagpur in 1999. He received his M.S. degree from Iowa State University, Ames, IA in 2002. From 2002 to 2005, he was a Ph.D. student at Georgia Institute of technology. He worked with Zenith Electronics from 2005 to 2006 before joining ArrayComm, LLC. His research interests include multiple antenna system design, cross-layer design, and statistical signal processing.